AD-A078 282 NAVAL POSTGRADUATE SCHOOL MONTEREY CA F/G 8/10
REPRESENTATION OF HYDROGRAPHIC SURVEYS AND OCEAN BOTTOM TOPOGRA--ETC(U)
SEP 79 A J PICKRELL

UNCLASSIFIED NL

1 OF 2
AD
A078282

NAVAL POSTGRADUATE SCHOOL
Monterey, California

THESIS

REPRESENTATION OF HYDROGRAPHIC SURVEYS AND OCEAN BOTTOM TOPOGRAPHY BY ANALYTICAL MODELS

by

Alan J. Pickrell

September 1979

Thesis Advisors: R. W. Garwood, Jr.
R. H. Franke

Approved for public release; distribution unlimited

SECURITY CLASSIFICATION OF THIS PAGE (When Data Entered)

REPORT DOCUMENTATION PAGE

READ INSTRUCTIONS BEFORE COMPLETING FORM

1. REPORT NUMBER

2. GOVT ACCESSION NO.

3. RECIPIENT'S CATALOG NUMBER

4. TITLE (and Subtitle)

(6) Representation of Hydrographic Surveys and Ocean Bottom Topography by Analytical Models.

(9) 5. TYPE OF REPORT & PERIOD COVERED
Master's Thesis, September 1979

6. PERFORMING ORG. REPORT NUMBER

7. AUTHOR(s)

(10) Alan J. Pickrell, LCDR, NOAA

8. CONTRACT OR GRANT NUMBER(s)

9. PERFORMING ORGANIZATION NAME AND ADDRESS
Naval Postgraduate School
Monterey, California 93940

(11) 10. PROGRAM ELEMENT, PROJECT, TASK AREA & WORK UNIT NUMBERS
Sep 79

11. CONTROLLING OFFICE NAME AND ADDRESS
Naval Postgraduate School
Monterey, California 93940

12. REPORT DATE

13. NUMBER OF PAGES
110

14. MONITORING AGENCY NAME & ADDRESS(if different from Controlling Office)
Naval Postgraduate School
Monterey, California 93940

(12) 111

15. SECURITY CLASS. (of this report)
Unclassified

15a. DECLASSIFICATION/DOWNGRADING SCHEDULE

16. DISTRIBUTION STATEMENT (of this Report)
Approved for public release; distribution unlimited

17. DISTRIBUTION STATEMENT (of the abstract entered in Block 20, if different from Report)

18. SUPPLEMENTARY NOTES

19. KEY WORDS (Continue on reverse side if necessary and identify by block number)
Hydrography, surface modeling, topographic modeling, analytical surfaces, ocean bottom topography

20. ABSTRACT (Continue on reverse side if necessary and identify by block number)
Hydrographic surveys for nautical charting contain many discrete data points. Analytical models for ocean bottom topography could save computer storage and reduce the complexity of automating the nautical charting process, but they must meet stringent accuracy requirements. Polynomials, double Fourier series, finite elements, Duchon's analysis, Shepard's formula, and Hardy's multiquadric analysis were investigated as possible modeling

DD FORM 1 JAN 73 1473 EDITION OF 1 NOV 65 IS OBSOLETE
S/N 0102-014-6601
(Page 1)

SECURITY CLASSIFICATION OF THIS PAGE (When Data Entered)

techniques. Multiquadric analysis in which the surface is represented by an analytical summation of mathematical surfaces such as cones and hyperboloids was the only method found to be suitable. An iterative method of model point selection was found to give the best results. Smooth and unambiguous junctions of adjacent models were made by using a Hermite polynomial weighted sum of overlapping areas. Highly irregular surfaces can be represented by about 20% of the original survey data points; more regular bottom topography can be represented by a smaller percentage.

Approved for public release; distribution unlimited

Representation of Hydrographic Surveys and Ocean Bottom Topography by Analytical Models

by

Alan J. Pickrell
Lieutenant Commander, NOAA
B. A., University of California at Los Angeles, 1971

Submitted in partial fulfillment of the
requirements for the degree of

MASTER OF SCIENCE IN OCEANOGRAPHY (HYDROGRAPHY)

from the

NAVAL POSTGRADUATE SCHOOL
September 1979

Author Alan J. Pickrell

Approved by: Roland W. Garwood Jr
Thesis Advisor

Richard Franke
Co-Advisor

Christopher N. K. Mooers
Chairman, Department of Oceanography

William M. Tolles
Dean of Science and Engineering

ABSTRACT

Hydrographic surveys for nautical charting contain many discrete data points. Analytical models for ocean bottom topography could save computer storage and reduce the complexity of automating the nautical charting process, but they must meet stringent accuracy requirements. Polynomials, double Fourier series, finite elements, Duchon's analysis, Shepard's formula and Hardy's multiquadric analysis were investigated as possible modeling techniques. Multiquadric analysis in which the surface is represented by an analytical summation of mathematical surfaces such as cones and hyperboloids was the only method found to be suitable. An iterative method of model point selection was found to give the best results. Smooth and unambiguous junctions of adjacent models were made by using a Hermite polynomial weighted sum of overlapping areas. Highly irregular surfaces can be represented by about 20% of the original survey data points; more regular bottom topography can be represented by a smaller percentage.

TABLE OF CONTENTS

LIST OF TABLES

LIST OF FIGURES

LIST OF FIGURES (cont)

ACKNOWLEDGEMENTS

I would like to express my sincere gratitude to Dr. R. W. Garwood and Dr. R. H. Franke, my advisors, for their assistance; Dr. R. L. Hardy for his timely response to my inquiries; Mr. Larry Mordock for his ideas on the topic and aid in obtaining survey data; and Mr. James Steensland and Lieutenant Maureen Kenny for supplying survey data.

I. INTRODUCTION

A. BACKGROUND

The ocean bottom is a continuous but generally irregular surface. In the deep oceans there are vast areas of abyssal plains interrupted by mid-ocean ridges, sea mounts and continents. The continental shelves and coastal areas vary from smooth flat bottoms to highly irregular surfaces with deeply gouged glacial troughs or coral and rock pinnacles. Many geological formations which are found on land such as canyons, mountains, domes, faults, etc., are also found on the continental shelves. The shape of the ocean bottom is difficult to determine since it cannot be seen or photographed except in very shallow areas and, direct measurement requiring occupation of the ocean bottom is costly and often impossible.

There are many reasons for which the shape of the ocean bottom must be known. Historically, safety of navigation has been the most urgent reason. Nautical charts are compiled from many sources to aid the navigator. These charts depict the coastlines and ocean bottom features using contour lines and selected depths.

The primary sources of depth data for nautical charts are hydrographic surveys. These surveys represent ocean bottom topography by discrete data points which are defined

by geographic position and depth below a specified water level datum. Until the mid-twentieth century, these depths were determined by lowering a weight on a calibrated line until it touched bottom. The vessel position was usually determined by measurements with sextants. Using these manual methods, data acquisition was very slow and only a minute percentage of the bottom was sampled. There were many sources of error in the observational procedures. A typical survey had a few hundred data points from which the surface shape between points had to be inferred. Data processing was easily handled by manual methods. More recently, electronic positioning equipment and depth sounding instruments have been used in semi-automated and automated systems. These systems allow almost continuous sampling of the ocean bottom along the vessel track. They have increased the accuracy of the data and the completeness of bottom coverage. As a result, depths need to be inferred between vessel tracks but not along the tracks. A typical survey of this type contains between 2,000 and 20,000 data points. These systems increased the data acquisition rate to such an extent that manual data processing methods could not keep up with data acquisition. Computer aided systems for processing and verifying the data were developed in the 1960's and 1970's.

Producing a nautical chart requires compilation of many hydrographic surveys, shoreline manuscripts, and other

documents. This remained a manual process until the mid 1970's. At this time, the National Ocean Survey (NOS) of the United States National Oceanic and Atmospheric Administration (NOAA) began development of a computer assisted chart compilation and production system (Moses and Passauer, 1979). This system requires on-line storage and manipulation of large blocks of discrete point data from hydrographic surveys. The density of these data from modern surveys make this a complex and costly process.

In an effort to produce one hundred percent bottom coverage for critical areas, multi-beam sounding systems (Hopkins and Mobley, 1978), airborne laser depth measuring systems (AVCO Everett Research Laboratory, 1978), and airborne water penetrating photography systems (Keller, 1976) have been developed. Some of these systems have proved that one hundred percent bottom coverage is feasible. They have also created another problem concerning representation of the data and its use in the compilation of nautical charts. The data from the multi-beam sounding systems for a typical survey would be equivalent to several hundred thousand discrete data points. Data from a laser system would be even more dense. The photogrammetric method uses stereographic images produced from aerial photographs. This can be considered to be truly continuous data, but such data is difficult to represent in a digital computer. The usual method to represent this data is to select the most representative and most critical depths for use as if they were from a

conventional survey. For a bottom with little relief, this method is satisfactory but as bottom relief increases, considerable detail and completeness is lost.

B. MATHEMATICAL MODELS FOR OCEAN BOTTOM TOPOGRAPHY

The density of data from modern hydrographic surveys has made the automation of chart compilation difficult. A possible solution to this problem which is investigated by this thesis is the use of a surface defined by an analytical expression to approximate the ocean bottom topography. Such a mathematical model would be used to compute a depth at any geographic position within the bounds of the model. In order to be useful, such a model must require considerably less data storage for the parameters which define the model than was required by the original set of discrete points.

The accuracy of the model is of utmost importance. The United States government can be held liable for vessel groundings or accidents at sea which are due to inaccurate charts. Special Publication 44 of the International Hydrographic Bureau (1968) states the accuracy specifications recommended for hydrographic surveys. The depth measurement specifications are listed in Table I.

Table I - Depth Measurement Specifications
Recommended by the International Hydrographic Bureau

Depth	Allowable error
0-20 meters (0-11 fathoms)	0.3 meters (1 foot)
20-100 meters (11-55 fathoms)	1.0 meters (0.5 fathoms)
Deeper than 100 meters	1% of depth

The Hydrographic Manual of the National Ocean Survey (Umbach, 1976) adds that accuracies attained for all hydrographic surveys conducted by the National Ocean Survey shall equal or exceed the specifications recommended by the International Hydrographic Bureau. These standards do not necessarily apply directly to the accuracy requirements for a mathematical model of the bottom, but they are good reference figures.

Solution of the dense data problem for nautical charting was the primary motivation for the investigation, but there are other uses for models approximating ocean bottom topography. Many coastal processes are closely related to bottom topography. These include wave height, wave refraction, energy dissipation, wave runup, storm surge and beach erosion. Design of offshore structures requires input of bottom characteristics. Subsurface, as well as surface navigation, could be aided by an ocean bottom model stored in an onboard computer. The accuracy requirements and model scales for these applications would be different but the modeling methods could be the same.

C. SCOPE OF WORK

There are several ways to represent surfaces by mathematical expressions. Those that seemed most applicable to the problem are discussed in Section II. Three of the models were chosen for experimental analysis. Portions of four hydrographic surveys conducted by the National Ocean Survey were used as experimental data sets for this analysis. These data sets represent a variation from extreme bottom relief to a very flat bottom. The models developed for these areas were analyzed quantitatively by comparing observed survey depths and computed model depths at the same location. Qualitative comparisons of depth contours from the two sources were also made. For each type of model, the input parameters were varied to investigate minimum requirements for a good representation.

Determining the exact location of the shoreline and other boundaries is an important part of any survey, but including this in the models is beyond the scope of this investigation. All the areas used for experimentation were restricted so that they do not include shoreline.

II. SURFACE MODELING METHODS

Analytical expressions have been used previously to approximate topographic surfaces. Some techniques used in map analysis are also applicable to the problem and there are some appealing methods which have been used for other surface approximations but not for terrain models. None of these methods have been used to represent hydrographic surveys. Ocean bottom topography is often similar to land topography but the research on terrain models has generally been for small scale large area maps. The large scale hydrographic surveys which must represent detail on the order of tenths of fathoms or feet are quite different than those large area maps, so modeling techniques which are good for small scale terrain models may not be appropriate for hydrographic survey modeling. Some important properties of the methods which must be considered aside from accuracy are:

- ease of computation - Must a large system of equations be solved to develop the model?
- dependence of horizontal scale - Hydrographic surveys and marine charts of different scales often overlap or are adjacent. For this reason, it is not good if the accuracy of a modeling method varies with horizontal distance scale.
- global versus local models - A global model represents a large area with a single expression. A local modeling

method represents many adjacent small areas with many corresponding expressions. Generally, there is more computation involved in global methods, whereas, local modeling requires more data searching to find the appropriate local parameters. Global models which attain significant data storage savings are of particular interest in this study.

- interpolation versus approximation - Interpolation methods generate a surface which fits some data points exactly and is used to interpolate between those points for surface values at other positions. Approximation methods generate a surface which approximates all the data but may not fit any data points exactly. A "best fit" by some criteria such as least squares is usually used. Approximation methods may not represent the least depth in an area accurately or they may move the position of peaks and deeps significantly. It is imperative that the model can be controlled to represent critical data points exactly. Interpolation methods are thus more appropriate for this application. The data points which are selected for interpolation will be called model points in this presentation. Quite often they are significant data points such as a least depth or an area of slope change.

The following sections discuss methods and previous research which are applicable to the problem.

A. POLYNOMIALS

Czegledy (1977), Hardy (1971), Krumbein (1966), and Whitten (1970), discuss the use of polynomials for surface representation. A polynomial mapping equation of two independent variables with a specified degree can be produced which fits a few data points exactly or approximates all the data in a least squares sense. In either case, the system of equations which must be solved becomes ill-conditioned as the degree of the polynomial increases. This can be alleviated by using orthogonal polynomials. In the method of orthogonal polynomials, a collocated series of independent surfaces, linear, quadratic, cubic, etc., is generated. The summation of these surfaces is the mapping equation which defines the model. Increasing detail is gained by solving for and adding the surface of next higher order. This method has proven useful for trend analysis of maps. However, it has been rejected by some investigators for applications requiring more accuracy. The reason as stated by Hardy (1971) is that the "ordinary collocated polynomial series is unmanageable in representing the sometimes rapid and sharp variations of real topographic surfaces." Requiring a high degree polynomial to fit closely spaced irregular surface points in one area causes significant invalid variations in other areas. To avoid these problems, low degree polynomials have been used in a local approximation mode with success, but this does not produce a global surface model.

B. DOUBLE FOURIER SERIES

The double Fourier series model is discussed by James (1966) and Krumbein (1966). It is produced by a series of independent harmonic surfaces having wave forms of diminishing wave length as the order of the surface increases. This technique has proven valuable for trend analysis particularly when the surface features show oscillating patterns. Unfortunately, the models require high order surfaces to represent sharp terrain features. Such surfaces produce oscillations with large variations between data points and have many of the same drawbacks as the collocated polynomial series.

C. FINITE ELEMENTS

Gold, Charters and Ramsden (1976) discuss a method of surface representation in which a system of triangles with data points at the vertices is imposed on a surface. An interpolating function is used to estimate the surface in each triangular element. The interpolant is developed so that the surface passes through the vertices and makes a smooth transition from one triangle to the next.

Peucker, Fowler, Little and Mark (1977) have developed a similar system of surface representation by Triangulated Irregular Networks (TIN). Rather than a smooth interpolant, the TIN system uses the planes defined by the three function values at the vertices of each triangle to represent the surface. Considerable work has been done on automated

techniques for selecting appropriate points to be used for vertices and on development of data structures for storage of the vertices, neighboring points, and neighboring triangles. The TIN system was developed specifically for digital representation of topographic surfaces.

Finite element systems such as these are local methods. Detail can be easily incorporated into the model by adding points where required without affecting the model elsewhere. Very little computation is required but searching the data structure to find the appropriate element is necessary. Such systems are generally independent of scale unless a scale dependent interpolant is used. A single expression which represents the surface is not generated by these methods.

D. SHEPARD'S FORMULA

Shepard's method as described by Poeppelmeier (1975), Barnhill (1977) and Franke (1979), has been widely used to interpolate random data but has never been used for topographic surface representation. The model is produced by taking a weighted average of the model points to interpolate the surface value at other points.

Shepard's formula is expressed by

$$f = \begin{cases} \dfrac{\sum_i w_i f_i}{\sum_i w_i} & \text{if } d_i \neq 0 \text{ for all } i \\ f_i & \text{if } d_i = 0 \text{ for any } i \end{cases} \qquad (1)$$

where the f_i are the depths at the model points; d_i is the distance from the ith model point to the point of computation; and the weight assigned to each model point, w_i, is a function of $\frac{1}{d_i}$. Two such weighting functions used in this project were simply the inverse distance ($1/d_i$) and the inverse distance squared ($1/d_i^2$).

In this method, all model points contribute to the value of f, but the effect of any model point on the interpolant decreases as the distance from that point increases. Another appealing feature of this method is that the value of f will always be between the minimum and maximum values of the model points.

Franke and Little's modification to Shepard's method restricts the weighted summation to only those model points within a radius R of the computation point. With this modification, the weighting function approaches zero as the distance approaches R and remains zero at distances greater than R. The modified Shepard's formula is expressed by

$$f = \begin{cases} \dfrac{\sum_i \dfrac{(R-d_i)_+}{Rd_i} f_i}{\sum_i \dfrac{(R-d_i)_+}{Rd_i}} & \text{if } d_i \neq 0 \text{ for all } i \\ f_i & \text{if } d_i = 0 \text{ for any } i \end{cases} \qquad (2)$$

or

$$f = \begin{cases} \dfrac{\sum_i \dfrac{(R-d_i)_+^2}{R^2 d_i^2} f_i}{\sum_i \dfrac{(R-d_i)_+^2}{R^2 d_i^2}} & \text{if } d_i \neq 0 \text{ for all } i \\ f_i & \text{if } d_i = 0 \text{ for any } i \end{cases} \qquad (3)$$

where

$$(R-d_i)_+ = \begin{cases} R-d_i & \text{for } d_i < R \\ 0 & \text{for } d_i \geq R \end{cases} \qquad (4)$$

The weighting functions $1/d_i$ and $\frac{(R-d_i)_+}{Rd_i}$ produce surfaces with cusps at the model points. The weighting functions $1/d_i^2$ and $\frac{(R-d_i)_+^2}{R^2d^2}$ produce surfaces with flat spots at those points. For higher order functions of $1/d_i$ these flat spots increase in size and the slopes between them become steeper. These properties are shown in two dimensions in Figure 1.

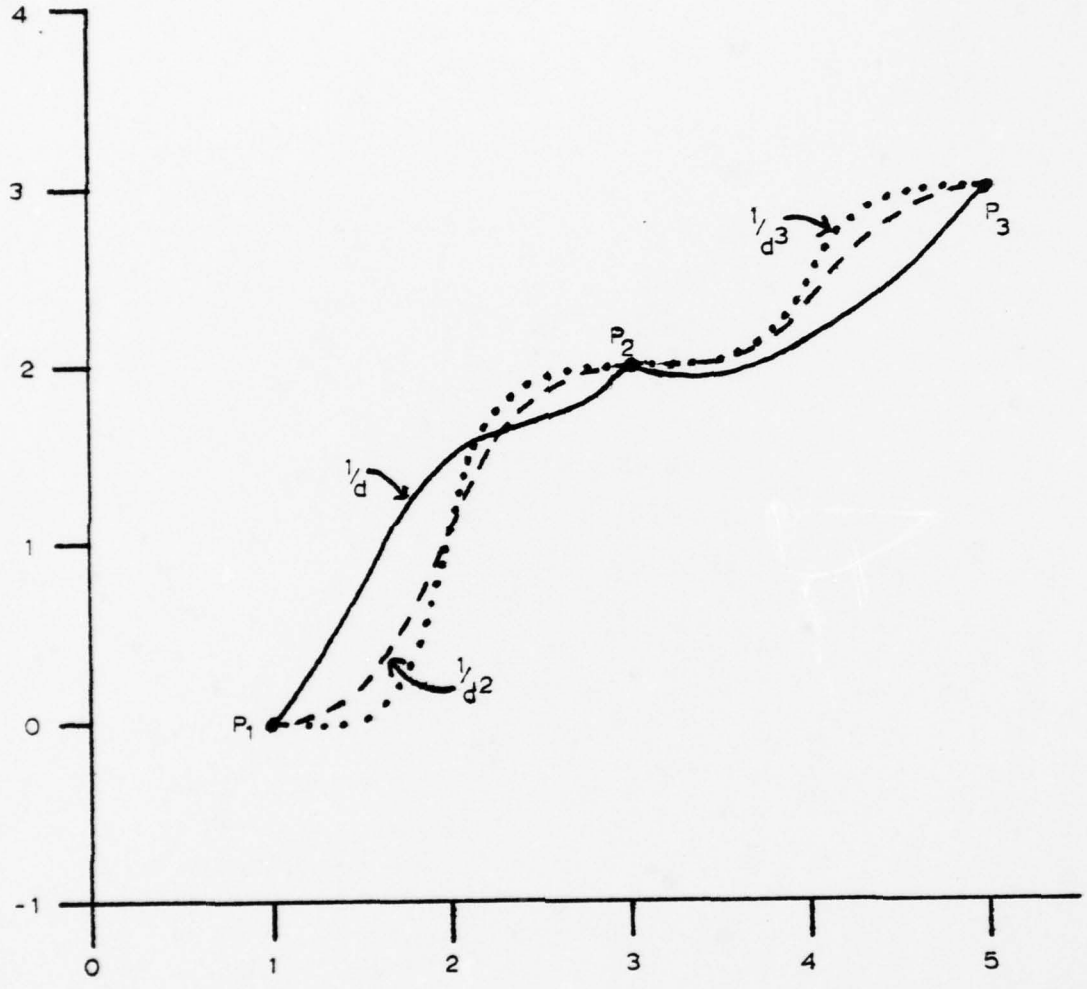

Figure 1 - Shepard's Formula with Various Weighting Functions

These formulas do not require solution of systems of equations and are easily modified by simply adding significant data points without recomputing any coefficients. They are independent of scaling, global in nature, and the computation is very simple.

E. DUCHON'S METHOD

The method of Duchon (1976) which was developed as thin plate surface theory is described by Meinguet (1979) and Harder and Desmarais (1972). It has never been used for topographic surfaces but has been used for other surface analyses. To develop this model, individual surfaces called basis or kernel functions, which are centered at the model points, are summed to yield a global surface. There is a coefficient associated with each kernel function which determines the magnitude of the effect of that kernel function on the total surface.

The expression for the model is

$$f = \sum_{i=1}^{n} C_i \left[F(X, Y, X_i, Y_i)\right] + A_1 + A_2 X + A_3 Y \quad (5)$$

where n is the number of basis functions and model points used. The last three terms represent a plane which is also added into the model. The n+3 coefficients C_i, i=1, ..., n, A_1, A_2 and A_3 are determined by solving the following system of n+3 equations.

$$
\begin{aligned}
f_1 &= \sum_{i=1}^{n} C_i \left[F(X_1, Y_1, X_i, Y_i)\right] + A_1 + A_2X_1 + A_3Y_1 \\
&\vdots \\
f_n &= \sum_{i=1}^{n} C_i \left[F(X_n, Y_n, X_i, Y_i)\right] + A_1 + A_2X_n + A_3Y_n \\
0 &= \sum_{i=1}^{n} C_i \qquad (6) \\
0 &= \sum_{i=1}^{n} C_iX_i \\
0 &= \sum_{i=1}^{n} C_iY_i
\end{aligned}
$$

where f_1, f_2, ---, f_n are the surface values at the model points (X_1Y_1) (X_2, Y_2), ---, (X_n, Y_n).

Duchon used two basis functions

$$
\begin{aligned}
&F(X, Y, X_i, Y_i) = d_i^3 \\
\text{and} \qquad &F(X, Y, X_i, Y_i) = d_i^2 \log d_i \qquad (7)
\end{aligned}
$$

where
$$d_i = ((X-X_i)^2 + (Y - Y_i)^2)^{\frac{1}{2}}. \qquad (8)$$

d_i is the horizontal distance from each model point to the point of computation.

Duchon's method using the above basis functions is independent of scale. During experimentation, a third basis function

$$F(X, Y, X_i, Y_i) = d_i \log d_i \qquad (9)$$

was also used. The models using this latter basis function are dependent on scale.

F. HARDY'S MULTIQUADRIC ANALYSIS

Multiquadric analysis, as discussed by Hardy (1971, 1972a, 1972b, 1975 and 1977) resulted from a search for a satisfactory and efficient method to represent topography by an analytical model. As suggested by its name, the method consists of summing many quadric surfaces (cones, hyperboloids, paraboloids, etc.), each associated with a model point, to obtain a global surface. Superficially, this method is similar to Duchon's method except that the kernel functions are quadric surfaces and the additioanl three terms are not used. The expression for this model is

$$f = \sum_{i=1}^{n} C_i \left[Q\,(X, Y, X_i, Y_i) \right] \qquad (10)$$

where f is the surface value at the point (X, Y); Q is the quadric surface or kernel function; (X_i, Y_i), i=1, ---, n are the model points at which the kernels are centered; and C_i, i=1, ---, n are coefficients assigned to each surface.

The following system of equations is used to solve for the unknown coefficients.

$$\begin{aligned} f_1 &= \sum_{i=1}^{n} C_i \left[Q\,(X_1, Y_1, X_i, Y_i) \right] \\ &\vdots \\ f_n &= \sum_{i=1}^{n} C_i \left[Q(X_N, Y_N, X_i, Y_i) \right] \end{aligned} \qquad (11)$$

The resulting surface will fit the data exactly at the model points (X_i, Y_i, f_i), i=1, ---, n.

Hardy (1971) found that the quadrics which yield the best reults are hyperboloids, cones and inverse hyperboloids.

A hyperboloid is represented by

$$Q(X, Y, X_i, Y_i) = ((X-X_i)^2 + (Y-Y_i)^2 + \delta^2)^{\frac{1}{2}}. \quad (12)$$

Cones are special cases of hyperboloids where δ is zero:

$$Q(X, Y, X_i, Y_i) = ((X-X_i)^2 + (Y-Y_i)^2)^{\frac{1}{2}} = d_i. \quad (13)$$

d_i is the distance from the point of computation (X, Y) to the center point of the each quadric surface (X_i, Y_i).

Inverse hyperboloid kernels are expressed by:

$$Q(X, Y, X_i, Y_i) = ((X-X_i)^2 + (Y-Y_i)^2 + \delta^2)^{-\frac{1}{2}}. \quad (14)$$

The magnitude of the coefficient C_i determines the steepness of the cone or hyperboloid. The sign of C_i determines whether the surface is oriented upward or downward. The magnitude of δ determines how flat the hyperboloid is at its center. These properties are shown in Figure 2.

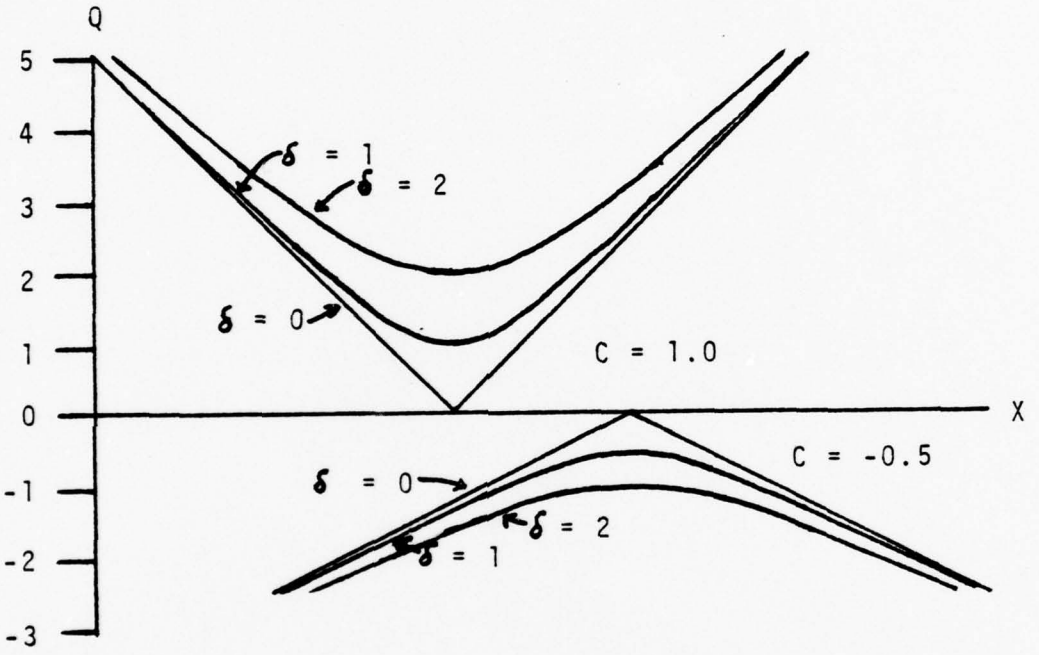

Figure 2 - Hyperboloid Kernels

For an inverse hyperboloid δ determines the peakedness of the surface at its center point (Figure 3). C_i simply represents a multiplicative constant which scales the size of the surface and specifies its orientation upward or downward.

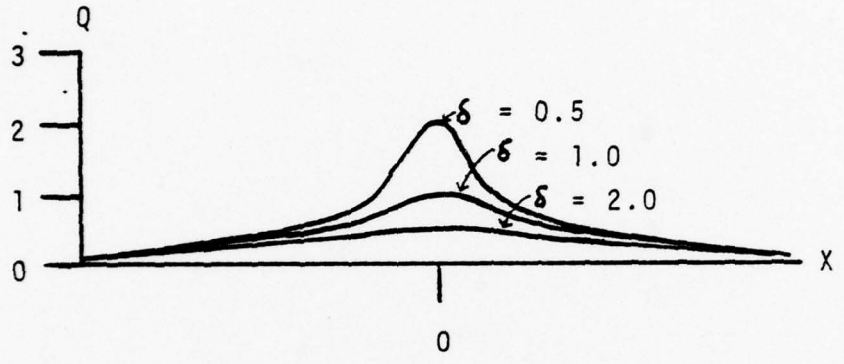

Figure 3 - Inverse Hyperboloid Kernels

For all C_i and δ the inverse hyperboloid approaches zero as the distance increases. There is an inflection point at $d = \delta/\sqrt{2}$.

The way several quadric surfaces sum to form the global surface can be seen in two dimensions in Figure 4.

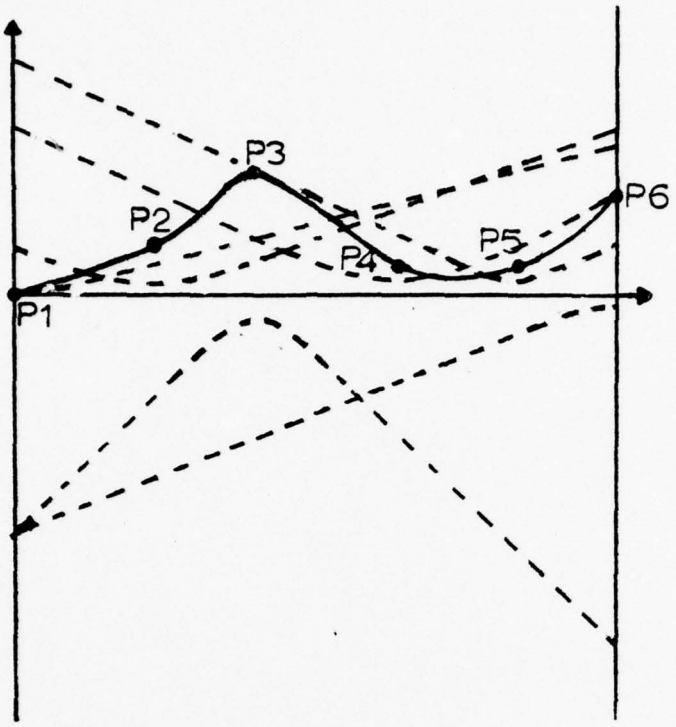

Figure 4 - Quadric Summations (hyperboloid kernels)

Multiquadric modeling is independent of horizontal scaling so long as δ is linearly related to the horizontal distance scales.

III. HYDROGRAPHIC SURVEYS

The data used in this project were from hydrographic surveys conducted in the late 1970's by the National Ocean Survey. The methods and procedures used were typical automated survey procedures as documented by Umbach (1976) and Wallace (1971). A brief description of these procedures followed by more specific information on each data set follows.

A. GENERAL DESCRIPTION

Safety of navigation is the primary purpose for which hydrographic surveys are accomplished. The data is acquired by running sounding vessels in parallel or nearly parallel tracklines on the ocean surface and taking depth measurements along these lines at evely spaced intervals. Crosslines are run at large angles to the main system of lines as a gross check on the validity of the data. When indications of critical bottom detail are found, development lines are run at closer spacing to determine the least depth and verify the nature of the feature. The depths are plotted on a survey sheet, a sample of which is shown in Figure 5.

There are many properties of a survey which affect its usefulness. Those most important to this project are survey scale, horizontal positioning accuracy and depth accuracy.

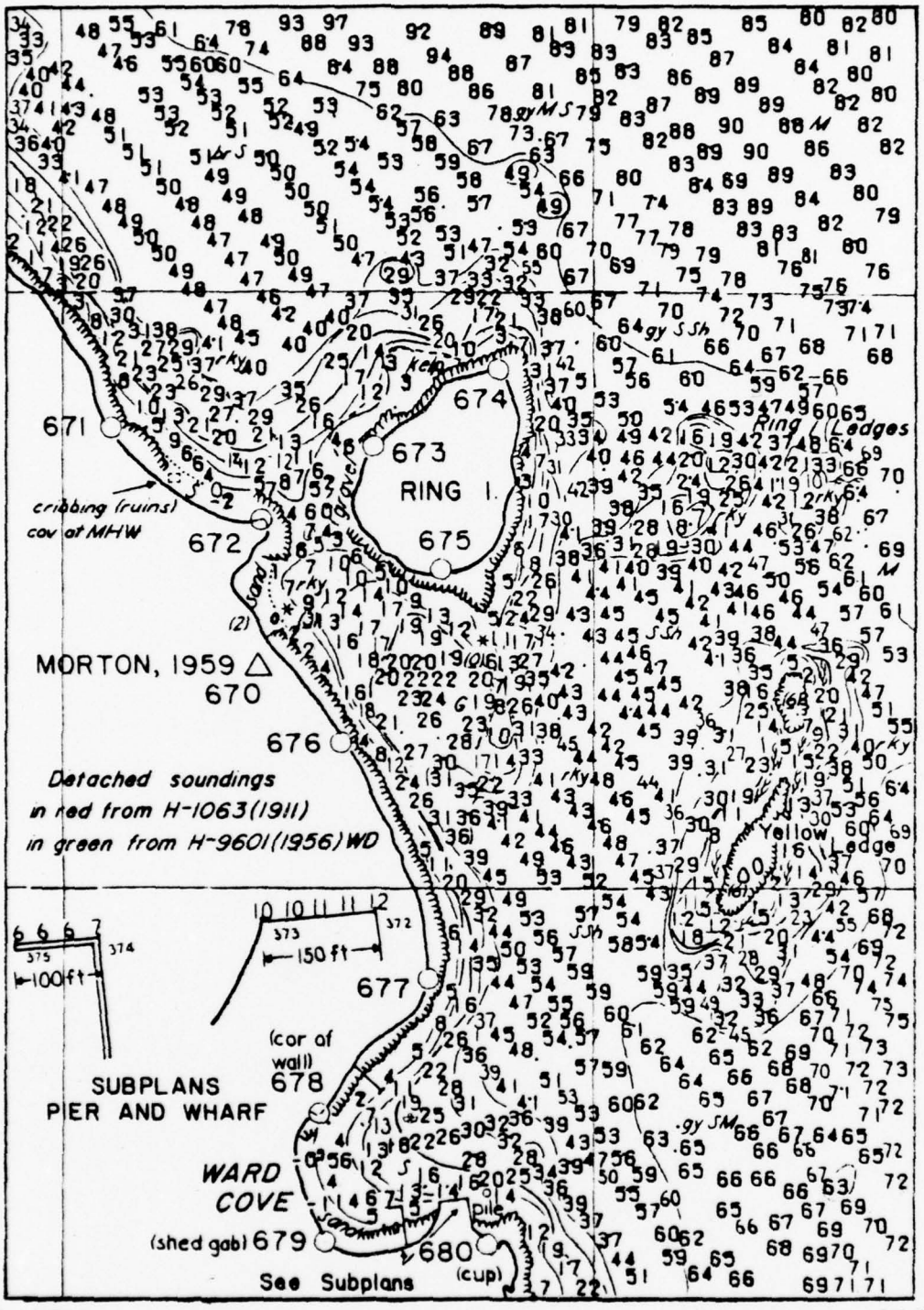

Figure 5 - Portion of a Hydrographic Survey Sheet

1. Survey Scale

The survey scale is the ratio of distance on the survey sheet to the corresponding distance on the earth. The scale chosen for a survey depends on "the area to be covered and the amount of detail necessary to depict adequately the bottom topography and portray the least depths over critical features." (Umbach, 1976) The survey scale is usually at least twice as large as the scale of any chart published for the area. Large scale surveys cover less area than small scale surveys but greater detail can be represented. For this reason, large scale surveys are conducted in harbors, anchorages, restricted navigable waterways, and areas where dangers to navigation are numerous. Areas with considerable detail are the most difficult to adequately represent by a mathematical expression. Three of the four data sets used in this project were from large scale surveys.

2. Horizontal Position Accuracy

Umbach (1976) specifies that plotted positions, "whether observed by visual or electronic methods, combined with plotting error shall seldom exceed 1.5 mm (0.05 in.) at the scale of the survey." On a 1:5000 scale survey, the position of each sounding should thus be represented to within 7.5 meters of its actual position on the earth. This is important in evaluating a mathematical model. One of the data sets had some very steep slopes, where an error

of a few meters in positioning would produce a depth variation of several fathoms. For areas such as these, a much greater depth discrepancy between the model and the survey data should be tolerable.

3. Depth Accuracy

As seen in Figure 6, there are many components that make up the depths represented in a hydrographic survey. In addition to the depth recorded by the sounding instrument, there are corrections for velocity of sound in the water column, the stage of the tide, and the dynamic vessel draft. Sometimes surveys have slight inconsistencies where data from two different vessels or two different days are adjacent or intermixed. These might be due to changes in the water column structure that affect the velocity of sound, an error in determining offshore tide corrections from tide gages near the shore, unrecorded changes in vessel speed affecting the dynamic vessel draft, a slight systematic error in vessel positioning, etc. Even more critical is the effect of waves on the sounding vessel. Small vessels change vertical position rapidly as waves pass while the instruments record the depth of the water column below the vessel. This depth is too great if the vessel is on a wave crest and too small if the vessel is in a trough. The angular orientation of the vessel is also affected by waves. If the vessel rolls to an angle greater than the sounding beam width, the depth recorded may not be under the vessel

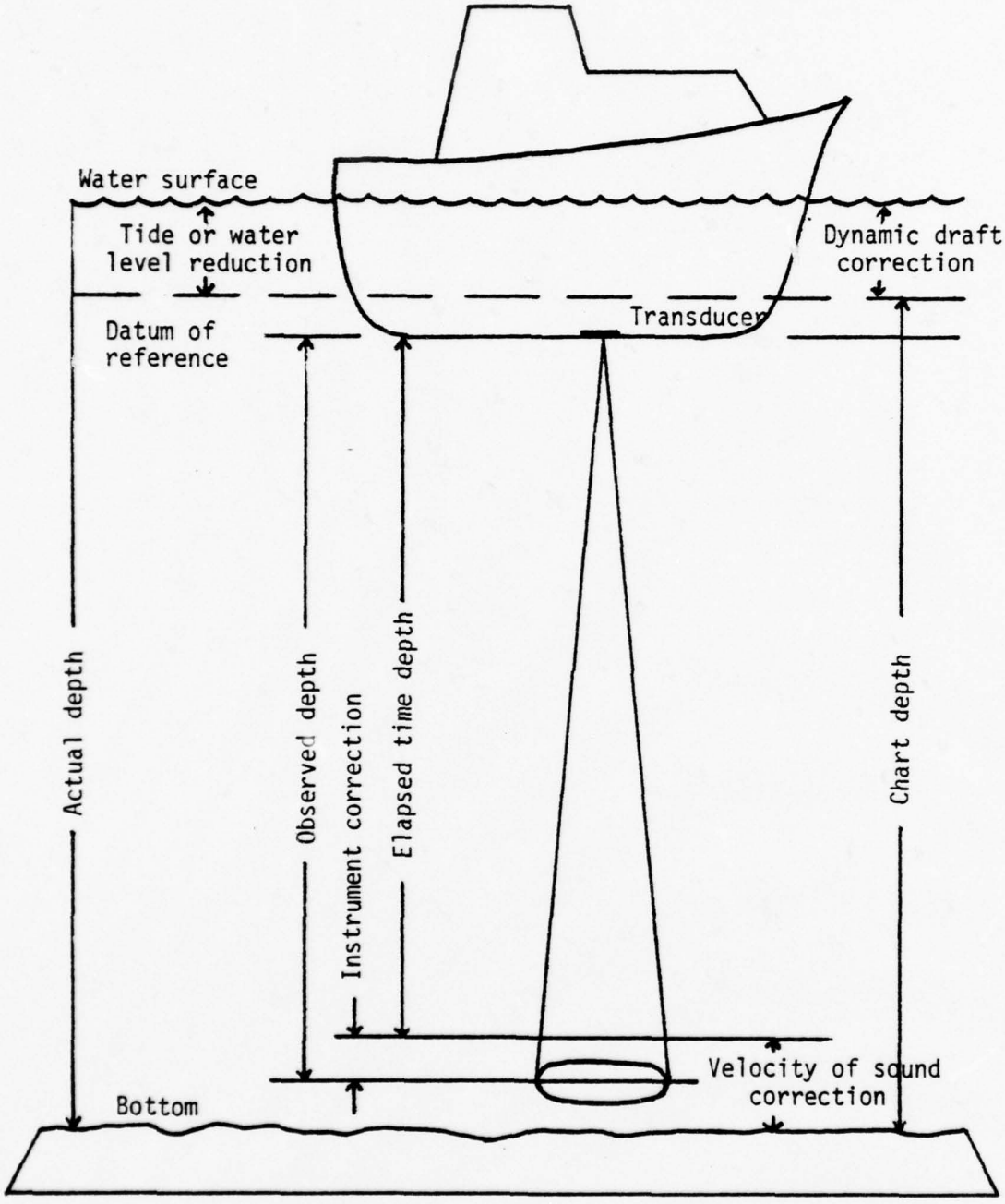

Figure 6 - Components of a Depth Measurement

but off to the side. In order to correct for this, the echograms were manually scanned, wave action was visually meaned out of the record, and depths that were automatically acquired with an error greater than the recording interval were rerecorded. On days of moderate to heavy wave action, this procedure leads to an inordinate amount of manual work introduced into an otherwise automated system. Table II indicates the depth recording and correction intervals used by NOS. Note that in many cases soundings from 0-20 fathoms need only be recorded to the nearest whole foot or nearest half of a fathom.

Although depth measurement errors can exist on all surveys, they are more apparent in areas of flat regular bottom. If two adjacent soundings each have nearly a foot of error of opposite sign, this will appear as a sharp discontinuity on a flat bottom whereas it will hardly be noticed on a steep slope. For this reason, models for areas of flat regular terrain when compared with the survey data may show some relatively large differences due to the data acquisition procedures.

B. DATA SETS

Four data sets were used for analysis in this project. They were specifically selected for the variety of bottom topography which they represent.

TABLE II - Depth Recording and Correction Intervals

Depth range (fm)	Character of area or bottom	For soundings scaled in feet				For soundings scaled in fathoms			
		In protected waters		In exposed waters		In protected waters		In exposed waters	
		Record soundings to the nearest	Apply corrections to the nearest	Record soundings to the nearest	Apply corrections to the nearest	Record soundings to the nearest	Apply corrections to the nearest	Record soundings to the nearest	Apply corrections to the nearest
0-20	Least depths over shoals and dangers	0.2	0.2	0.5	0.2	0.1	0.1	0.1	0.1
	In channels, established sea lanes, and fairways								
	Delineation of appropriate low water line								
	Elsewhere, over regular bottom	0.5	0.2	1.	0.5	0.1	0.1	0.2	0.1
	Elsewhere, over irregular bottom	1.	0.5	1.	0.5	0.2	0.1	0.5	0.2
20-110	Over regular bottom	1.	1.	1.	1.	0.2	0.1	0.5	0.2
	Over irregular bottom	2.	1.	2.	1.	0.5	0.2	1.	0.5
Greater depths	All bottom types	2.	1.	2.	1.	1.	1.	2.	1.

1. Monterey Bay, California

This data set was taken from survey registry number H-9808. It was conducted in 1979 by NOAA Ship DAVIDSON and Naval Postgraduate School personnel and equipment. It covers the southernmost part of Monterey Bay including Monterey Harbor. The survey was conducted at a scale of 1:5000. Only one vessel was used on the portion of the survey chosen for analysis. The sounding units are fathoms and depths range from 0 to 16 fathoms. The bottom has a large amount of detail. It slopes moderately downward from the shore and consists generally of mud and sand. In the middle there is an area thick with kelp which is attached to a rocky irregular bottom. There are a few rocky areas in the deeper part as well. Figure 7 shows the bottom contours in one fathom increments. The scale of the plot has been reduced for presentation herein.

2. Morro Bay, California

This data set was taken from survey registry number H-9737. It was conducted in 1978 by the NOAA Ship FAIRWEATHER. It covers a small part of Morro Bay and some navigable waterways open to the bay. The survey was conducted at a scale of 1:5000. The sounding units are feet and depths range from 16 to 82 feet in the portion used for analysis. Figure 8 (reduced scale) shows the bottom contours in three foot increments. There is one major feature near the center and considerable irregularity in the northeast corner of the area. Otherwise, the bottom slopes gently offshore.

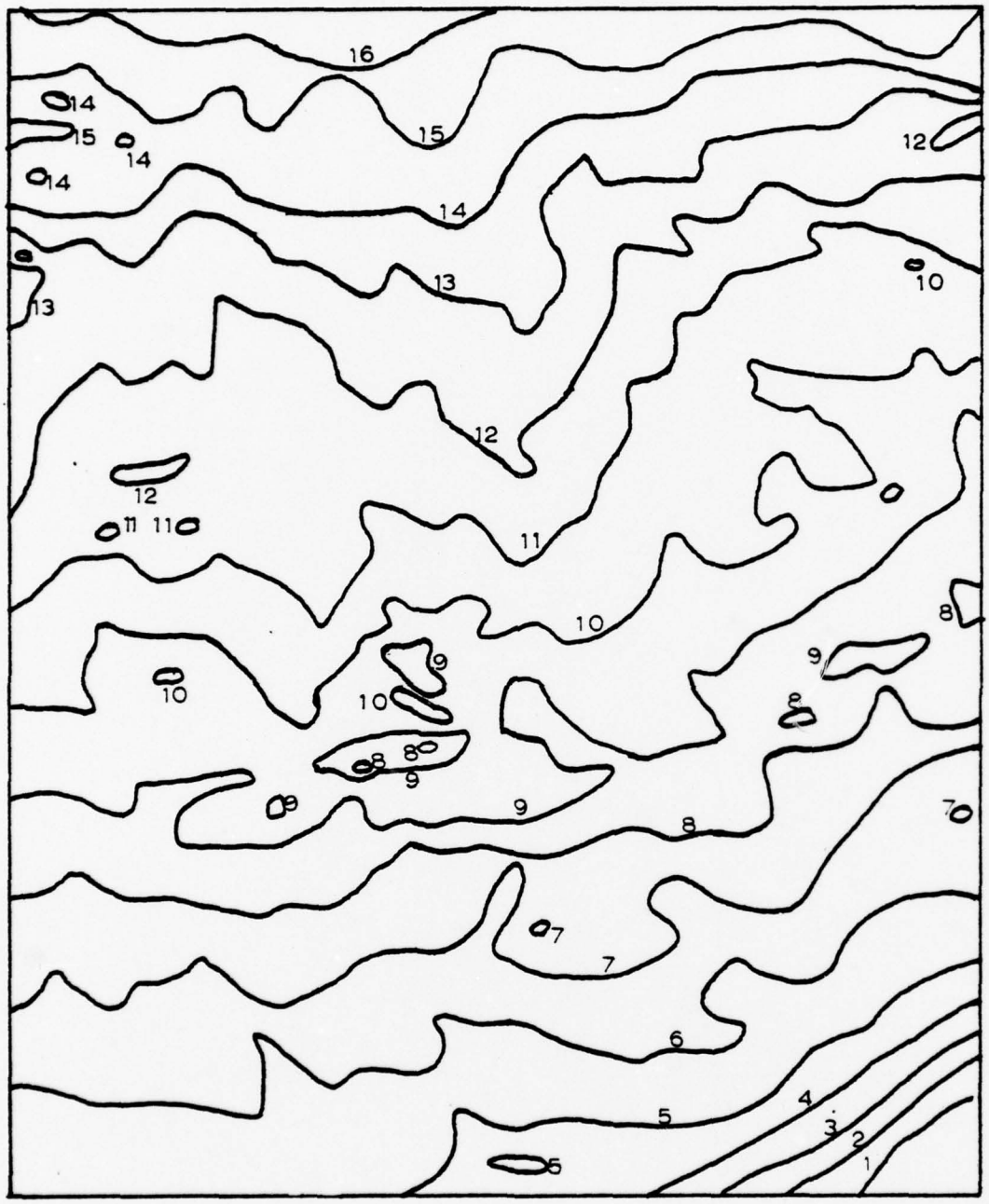

Figure 7 - Monterey Bay Data Set Contours (fathoms)

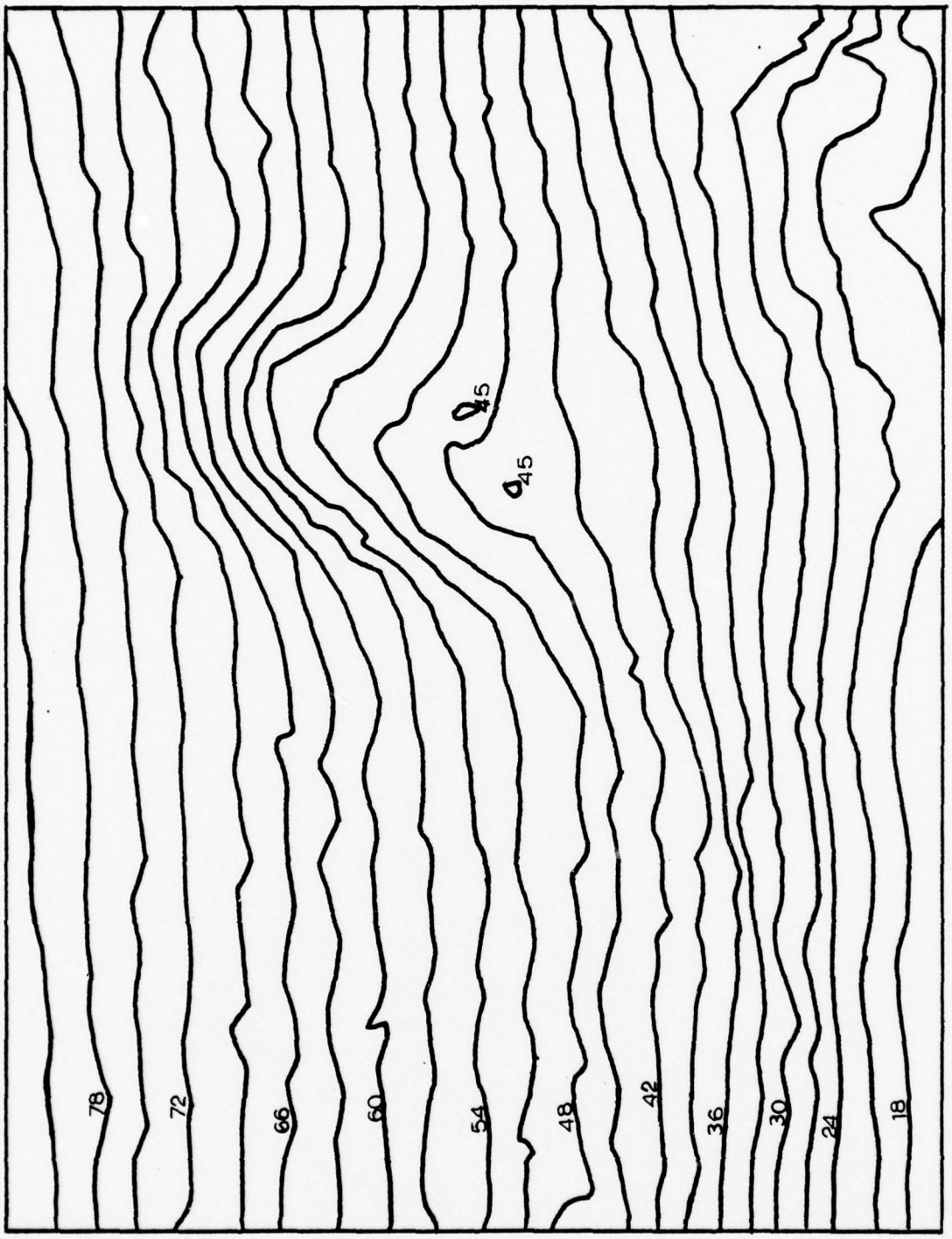

Figure 8 - Morro Bay Data Set Contours (feet)

3. Auke Bay, Alaska

This data set came from a thesis project by Seidel (1979), a student at the Naval Postgraduate School, which investigated the affects of using multiple sounding beam widths for hydrographic surveys. The procedures were somewhat non-standard since sounding lines were run much closer than normal in an attempt to gain 100% bottom coverage. Specifications for 1:5000 scale surveys were used but due to the dense sounding spacing, it was plotted at a scale of 1:2500. The data was incorporated into survey registry number H-9818. It was conducted in 1979 by Seidel and the NOAA Ship RANIER. It covers a small portion of Auke Bay in southeast Alaska. The sounding units are fathoms and depths range from 0 to 24 fathoms. The bottom is mostly mud and rock and shows a tremendous amount of variation due to glacial action. Very steep slopes are encountered in the area. At one point, the depth changes from 7 to 22 fathoms in a horizontal position change of only 30 meters. Figure 9 (reduced scale) shows the bottom contours of the central part of the data set in one fathom increments.

4. Gulf Coast

The fourth data set was taken from survey registry number H-9785. It was conducted in 1978 by the NOAA Ship MT MITCHELL at a scale of 1:20000 and covers an area in the

Gulf of Mexico off the coast of Louisiana. The sounding units are feet and depths range from 29 to 37 feet in the portion used for analysis. Figure 10 (reduced scale) shows the bottom contours in one foot increments. The bottom is generally flat with a very gentle slope. It consists mostly of mud and shell fragments. Some of the irregularities seen in the bottom contours are in areas where the work of two vessels overlapped because of crosslines or junctions. The flat bottom and small contour increment make these irregularities stand out. The survey party reported that wave action was also a considerable problem during the conduct of this survey.

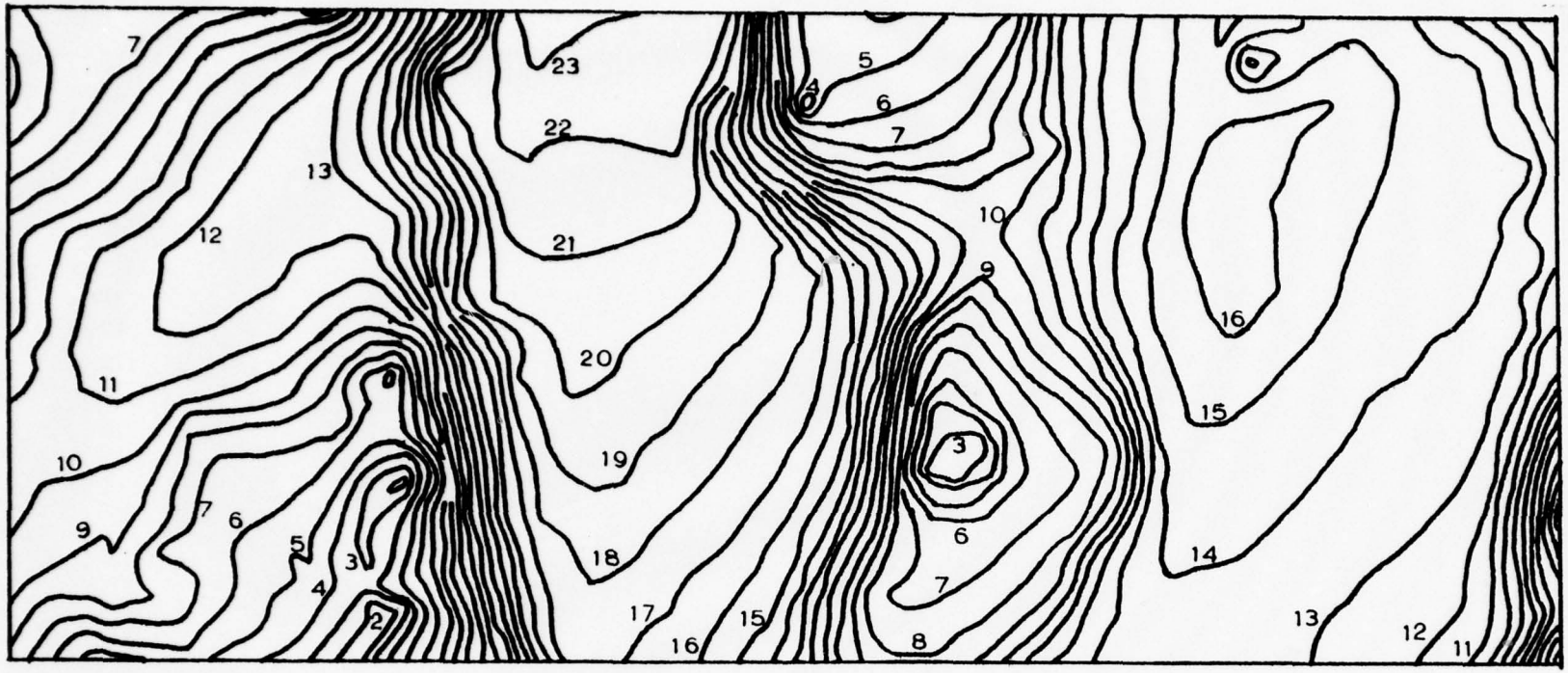

Figure 9 - Auke Bay Data Set Contours (fathoms)

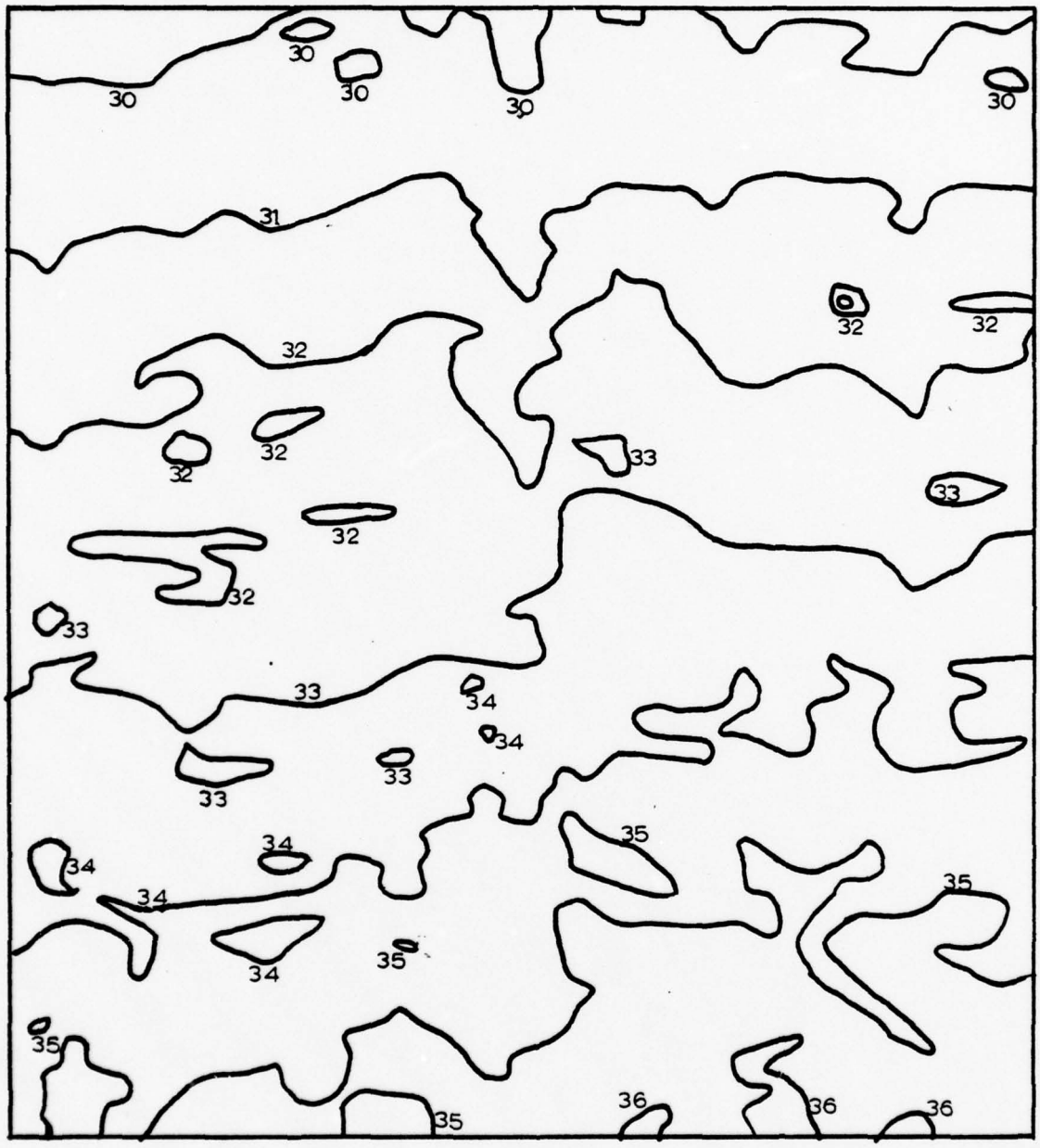

Figure 10 - Gulf Coast Data Set Contours (feet)

IV. RESEARCH PROCEDURES

A. COMPUTER SYSTEM

All the computer work for this project was done on the IBM 360/67 system at the Naval Postgraduate School's W. R. Church Computer Center. All programs were written in FORTRAN IV. The VERSATEC-07 electrostatic plotter was used for all the data and contour plotting. Both IMSL (International Mathematical and Statistical Library) routines and other library routines were used in the programs.

B. DATA SET PREPARATION

1. Original Data Condition

All four data sets were supplied by the National Ocean Survey on non-labeled unblocked magnetic tapes in the NOS standard record format. Positions of all soundings were given in terms of latitude and longitude. Corrected soundings were supplied to the nearest tenth of feet or fathoms. Each data point had a record sequence number assigned. The NOS format also included original observed data and all corrections to it as well as descriptive cartographic codes and other information.

2. Program TAPCNV - Tape Conversion

Only corrected position, corrected depth and record number identification were required for this project. The program TAPCNV was written to read this data from the non-labeled NOS tapes. The geodetic positions were converted to an X-Y plane coordinate system based on the Modified Transverse Mercator (MTM) projection (Wallace, 1971). Double precision computations were used for this conversion. The MTM projection gives the positions in terms of meters of northing and meters of easting from a local origin. This X, Y position was then converted to plotter coordinates in terms of inches from the plotter origin. The record number, depth, geodetic position, MTM coordinates and plotter coordinates were blocked and recorded on disk and on an NPS tape with standard system labels.

3. Program DATPLT - Data Plotting

This program was written to display the discrete point data on a plotted sheet. Latitude and longitude grid intersections at specified intervals were converted to plotter coordinates and straight lines were drawn connecting these points to provide the geodetic position reference system. Two sheets were plotted with this reference grid. On one sheet depths were plotted to the nearest tenth. (NOS plots tenths only in shallow water when the depth units are fathoms.) Record numbers were

plotted on the second sheet. Overlaying the two sheets facilitated reference to any particular data point. DATPLT was used to plot the entire surveys as a first step. When portions of the surveys were selected for analysis DATPLT was used again to select and plot only the data within the specified area.

4. Program CONDAT - Data Contouring

Part of the data analysis consisted of comparing contours of the original data with contours from the model. Initially, contours of the survey data were hand drawn - a procedure that is somewhat subjective. In order to remove as much subjectivity as possible from the analysis hand contouring was replaced by machine contouring. The library routine CONISD, for contouring irregularly spaced data, was used in the program CONDAT. This routine first generates triangles with data points at the vertices. By linearly interpolating along the triangle sides for the contour values, points on each contour are found and connected to generate the contour lines. The contours generated in this manner were not smooth as would be desirable, but the data points were dense enough so that this was not a problem.

C. MODEL DEVELOPMENT AND ANALYSIS

Program MODEL was written to do the model development, the quantitative analysis, and to aid in the qualitative

analysis. To change from one modeling technique to another the only modification necessary was the replacement of one module. That module contained the routine to develop the model by a given method and to compute the depth at any point. All the modeling techniques required the selection and use of model points from the survey data. The model points were specified by record numbers on punched card input and the survey data was read from disk and stored in memory. The model points were stored in arrays for model development.

1. Coefficient Computation - Subroutine LEQ2S

The methods of Hardy and Duchon require solution of symmetric systems of linear equations to determine the model coefficients. The double precision version of the IMSL routine LEQ2S was used for this purpose. This routine uses symmetric decomposition with iterative improvement to solve the systems. Systems of up to 226 equations in 226 unknowns were solved during the course of this project. The model coefficients and respective model points were output for analysis.

2. Quantitative Analysis - Subroutine STAT

Subroutine STAT was developed to provide a quantitative analysis of each model. Each survey depth was compared with the depth computed from the model at the same X, Y position. The root mean square difference, maximum positive difference and maximum negative difference were

tabulated for each run. A positive difference signified that the model depth was deeper than the survey depth; a negative difference signified that the survey depth was deeper. The root mean square difference is given by the expression

$$\text{RMS difference} = \left(\frac{\sum_{i=1}^{N} (MD-SD)^2}{N} \right)^{\frac{1}{2}} \qquad (15)$$

where MD is the model depth, SD is the survey depth, and N is the number of points used for the comparison. Those points with a difference greater than 1.5 times the RMS difference were listed for manual inspection and analysis.

3. Qualitative Analysis - Subroutines SETCON and CONTUR

The qualitative analysis was accomplished by comparison of model contours with those from the original data. In order to produce the model contours subroutine SETCON developed a quarter inch grid over the modeled area at the scale of the survey. The model depth was computed at each grid intersection. These depths and positions were passed to the library routine CONTUR for contouring. CONTUR is similar to CONISD except that it was written specifically for gridded data and runs considerably faster than CONISD.

V. RESEARCH RESULTS

A. SELECTION OF METHODS FOR EXPERIMENTATION

Of the modeling techniques discussed in Section II, Duchon's method, Shepard's formula and Hardy's multiquadric analysis were selected for testing. Neither Duchon's method nor Shepard's formula had previously been used for terrain surfaces. Multiquadric analysis had been used with good results for topographic data but not at the scales and accuracy requirements necessary for hydrographic survey representation.

The methods of polynomials and double Fourier series were not tested. They had proved to be useful for some applications such as trend analysis and representation of repeated features. The fact that forcing polynomials or double Fourier series to fit irregular data in small areas produces unwanted irregularity in other areas would seem to preclude these methods from producing good results in this application. Some methods reduce this effect by using local expressions which fit only small areas at a time, but this defeats the purpose of generating a global model to represent large areas of the data.

Finite element methods were not tested. They are strictly local methods which, in addition to storage of model points, require storage of pointers to the neighboring points and neighboring triangles of each model point.

B. METHOD COMPARISON PROCEDURES

The Monterey Bay and Morro Bay data sets were used for comparison of the methods. The Monterey Bay data set was used in the qualitative manner only. The Morro Bay data set was used for both qualitative and quantitative comparison. The procedures described below were used for all methods in order to make controlled comparisons.

As a first step, 42 data points on a 6x7 grid were chosen from the Monterey Bay data at regular spacing without regard to bottom detail. After the models were generated with these points, an additional 18 model points were selected in areas where more detail was required. Models were then generated using the 60 points. The third step was to choose 30 more points around the outside of the original area at the same spacing as the original 42 points extending the grid to 8x9. Models were generated with the 90 points to determine the affect of extending the model area.

Thirty-seven model points were chosen at regular spacing from the Morro Bay data set in the first step with that data. Thirty and thirty-one additional points were selected in the second and third steps for totals of 67 and 98 model points. The additional points were all within the original area in places where additional detail or accuracy was needed. The effect of increasing the model point density was examined in this way. The statistical results, as well as contours of the Morro Bay tests, were compared.

C. RESULTS OF DUCHON'S METHOD

Equation 5 shows that Duchon's model is produced by the summation of a plane and a series of basis functions centered at the model points. Duchon's method with the basis functions d^3 and $d^2 \log d$ and a similar method with basis function $d \log d$ were tested.

1. General Findings

For all three basis functions the 42 Monterey Bay points produced similar models which showed the general trend of the bottom but very little detail. Using the 60 model points, the basis functions d^3 and $d^2 \log d$ gave more detail and a fair representation of the bottom trends. See Figure 11.

The basis function $d \log d$ gave a very poor representation of the bottom when the 60 points were used. In an effort to resolve detail in some areas, several points were chosen very near each other. This caused steep slopes to be generated which extended into areas where there were no model points and created invalid peaks and deeps.

The quantitative results of Duchon's method using the Morro Bay data set are given in Table III. Note that the model using the basis function $d \log d$ became better in both RMS difference and maximum difference as the number of points was increased. The results didn't change much using the basis function $d^2 \log d$ and they became worse for the basis function d^3. The contours reflected these

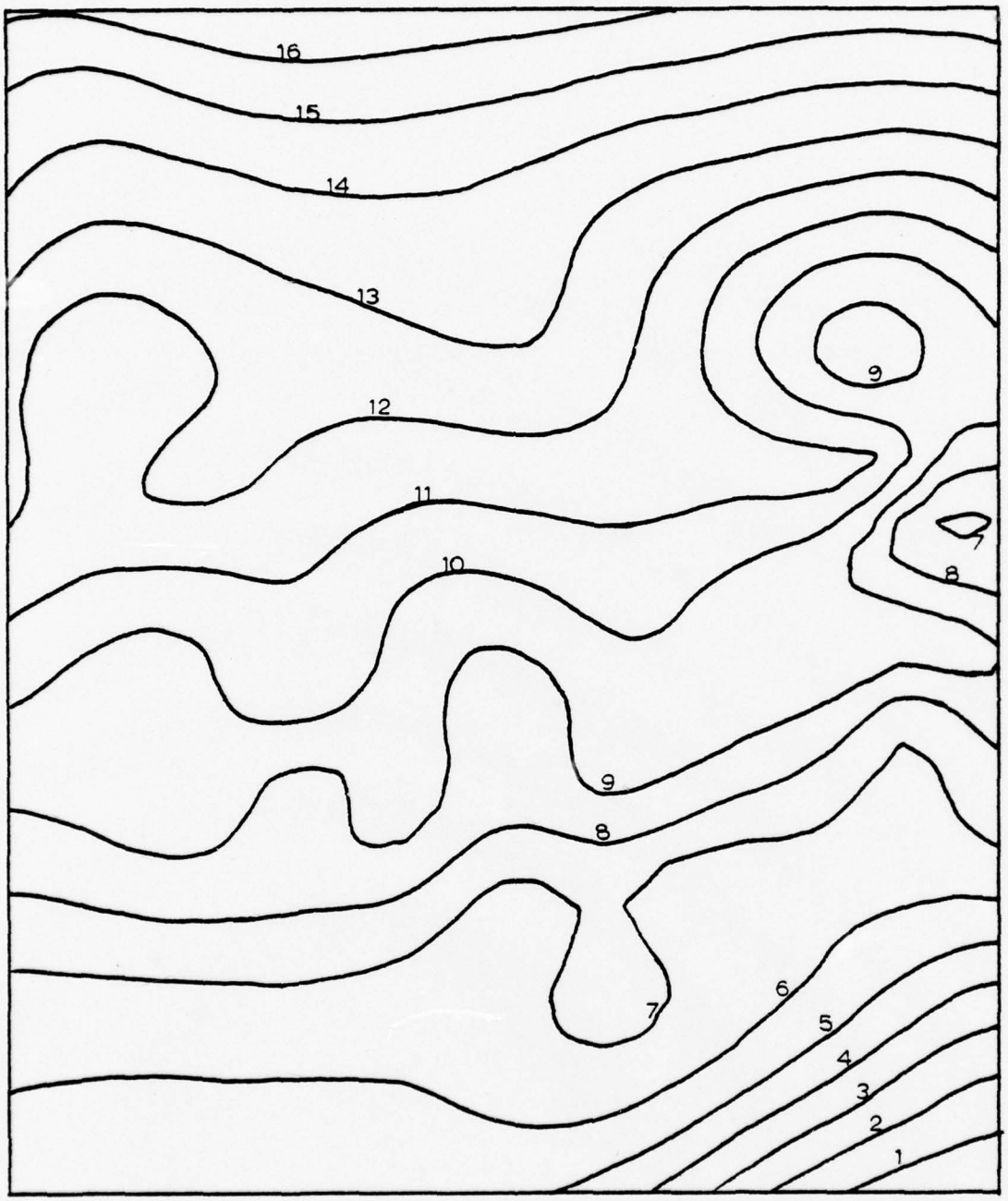

Figure 11 - 60 Point Duchon Model of Monterey Bay
(basis function $d^2 \log d$)

statistics. In the cases of the d^3 and d^2 logd basis functions, the detail was increased in the areas where points were added but the statistical results did not improve due to greater error in other areas. As shown in Figure 12, the model using 98 points with the basis function d logd compares very favorably with the original data contours in Figure 8.

TABLE III - Results of Duchon's Method - Morro Bay

Basis Function	Nr of model points	RMS difference	Maximum positive difference	Maximum negative difference	Nr of data points
d^3	37	1.20	3.89	-6.15	936
d^2logd	37	1.14	3.78	-6.29	936
d logd	37	1.15	4.32	-6.51	936
d^3	67	1.77	6.74	-7.99	936
d^2logd	67	1.11	4.09	-4.42	936
d logd	67	0.77	3.11	-3.15	936
d^3	98	2.13	7.75	-17.83	936
d^2logd	98	1.14	4.19	-6.15	936
d logd	98	0.67	2.23	-2.48	936

2. Dependence on Scale

The results of the previous section lead to a question concerning the ability of the basis function d logd to produce a much better model than other basis functions in one case but not in the other. The reason for this turned out to be the scale of the data. The first two basis

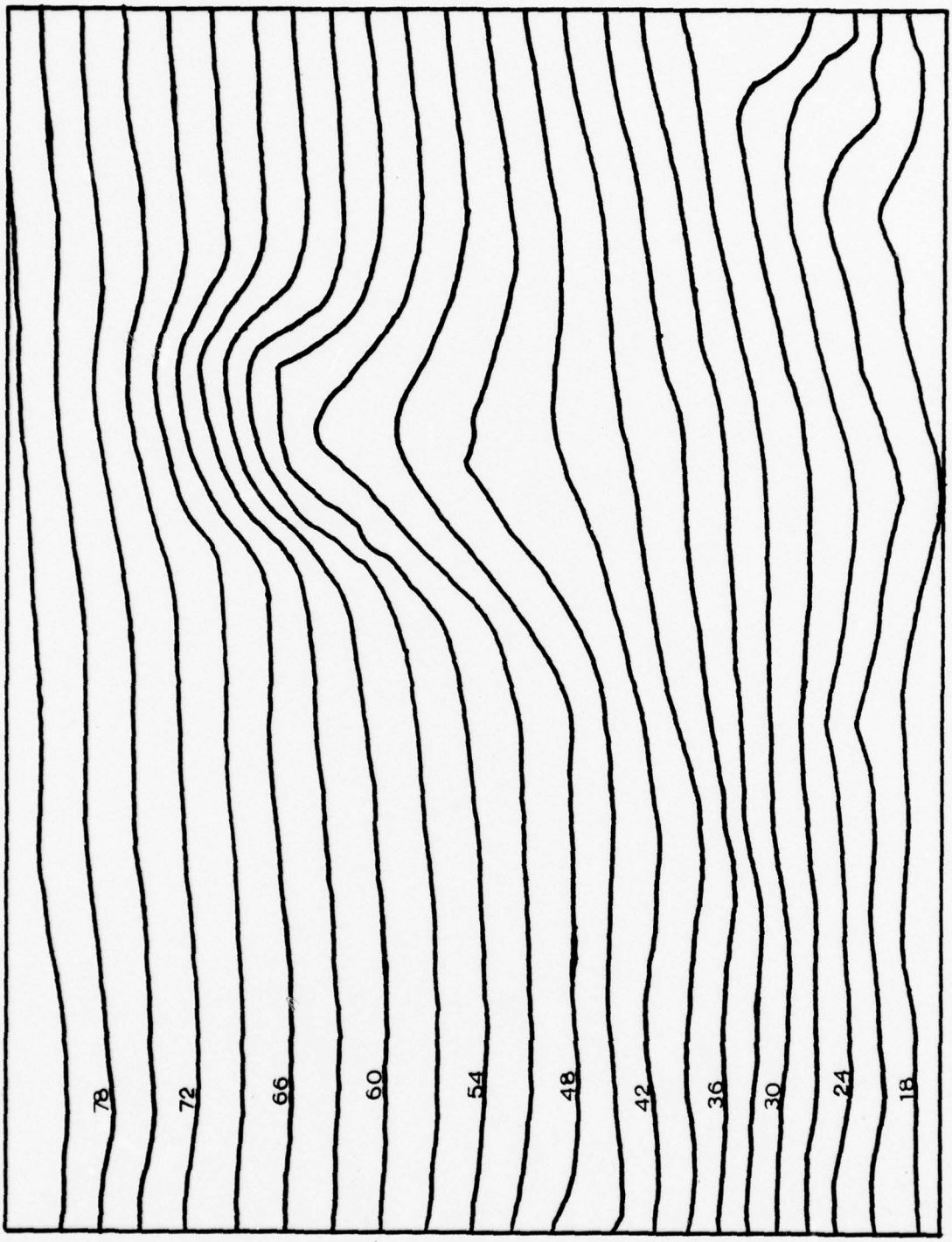

Figure 12 - 98 Point Model of Morro Bay
(basis function d log d)

functions produce models which are independent of scale whereas, the third produces models which are not. Initially, the Morro Bay data was used at the earth's natural scale in meters. At this scale, the system of equations was ill-conditioned to such a degree that it couldn't be solved. The data presented in the previous section was acquired with the horizontal position data scaled to a distance of unity on a diagonal from one corner of the area to the opposite corner. In this case, the results were good. The Monterey Bay data was scaled for a diagonal distance of 50. The results in this case were poor. Table IV gives the results of some tests run at various scales using the Morro Bay data and the basis functions d logd and d^2logd. The set of 98 model points and 936 data comparison points were used for these tests.

TABLE IV - Effects of Scale on Duchon's Method - Morro Bay

Basis function: d logd

Diagonal distance	RMS difference	Maximum positive difference	Maximum negative difference
0.001	0.675	2.115	-2.365
0.01	0.672	2.121	-2.379
0.1	0.668	2.131	-2.406
1.0	0.671	2.216	-2.479
10.0	5.829	13.566	-20.285
100.0	17.394	65.291	-198.561
1000.0	0.781	2.211	-2.461
Basis function:	$d^2 \log d$		
0.001	1.138	4.186	-6.149
0.01	1.137	4.185	-6.143
0.1	1.139	4.193	-6.155
1.0	1.138	4.189	-6.151
10.0	1.138	4.189	-6.151
100.0	1.138	4.189	-6.151
1000.0	1.138	4.190	-6.153

D. RESULTS OF SHEPARD'S METHOD

As defined in equation 1, Shepard's formula is a weighted summation of the model point depths. The weight assigned to each model point is a function of the inverse distance from the point of computation to the model point. The weighting functions used in this analysis were:

- $\frac{1}{d_i}$
- $\frac{1}{d_i^2}$
- $\frac{(R-d_i)_+}{Rd_i}$
- $\frac{(R-d_i)_+^2}{R^2 d_i^2}$

where $(R-d_i)_+$ is defined in equation 4.

1. Computation of R

In the modified Shepard's method, a radius of influence, R, is used. Rather than choosing this radius arbitrarily, a method was used which related R to the density of the model points independent of the scale of the data. This also allowed variation of R according to the average number of model points which would fall within the radius of influence.

The following expression was used for this purpose:

$$R = \sqrt{\left(D/2\right)^2 \frac{NPPR}{N}} \qquad (16)$$

where D is the maximum distance between any two model points, N is the total number of model points, and NPPR is the average number of points which should fall within the radius of influence. $\left(D/2\right)^2$ is related to the size of the area which contains the data points. Dividing this by N gives a measure of the average area which could be assigned to each point. Multiplying by NPPR gives the area which could be associated with that many data points. Taking the square root of this gives a radius which would define that amount of area centered at the point of computation. On the average there should be NPPR model points within a distance R from any point of evaluation. The tabulated statistical results express the radius in terms of NPPR instead of R.

2. Inverse Distance Weighting Function

Table V gives the statistical results of the tests using the inverse distance weighting functions. The table shows that use of the modified Shepard method improved the results considerably. In all cases, the best results were obtained by including an average of six model points in the radius of influence. The table also indicates that no statistical improvement was made by increasing from 37 to 98 model points.

The contours produced by this method (Figure 13) for both data sets were poor. The basic trend of the bottom can hardly be seen. The contours are quite wavy where they

TABLE V - Shepard's Formula with Inverse Distance Weighting Function - Morro Bay

Number of model points	NPPR	RMS difference	Maximum positive difference	Maximum negative difference	Number of data points
37	6	2.06	8.17	-9.37	936
37	9	2.28	7.33	-9.68	936
37	All*	10.88	24.43	-25.96	936
67	4	2.45	8.50	-7.97	936
67	6	2.17	5.69	-6.94	936
67	9	2.31	6.86	-7.61	936
67	25	3.53	9.61	-12.68	936
67	All*	11.41	22.77	-28.58	936
98	4	2.41	8.11	-8.95	936
98	6	2.17	7.37	-6.73	936
98	9	2.22	8.64	-7.51	936
98	25	3.46	11.38	-12.51	936
98	56	5.03	13.33	-16.50	936
98	All*	12.50	21.33	-32.22	936

* Shepard's formula - All model points contributed to the weighted average.

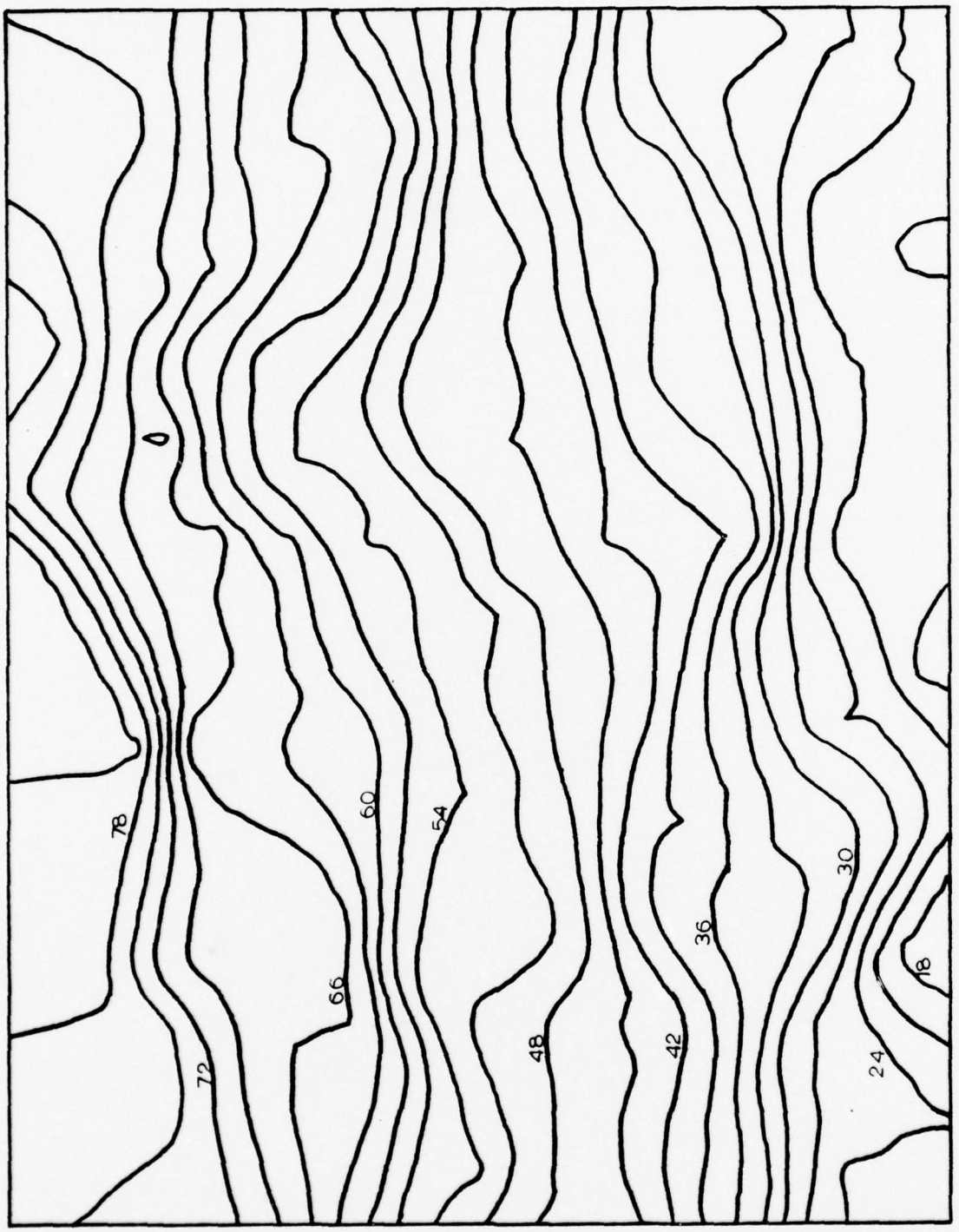

Figure 13 - 98 Point Shepard's Formula Model of Morro Bay
(NPPR = 6)

should be straight. In some cases, peaks or deeps are produced at the positions of model points which aren't found in the original data.

3. Inverse Distance Squared Weighting Function

Table VI gives the statistical results of similar tests using the inverse distance squared weighting function. There is considerably less variability as NPPR is changed using this weighting function. The results are better for large NPPR and for the unmodified version, but the best results at smaller NPPR did not improve.

E. RESULTS OF HARDY'S MULTIQUADRIC ANALYSIS

As indicated in equation 10, Hardy's multiquadric model is generated by summing quadric kernel surfaces, each of which are centered at model points. Hyperboloids, cones and inverse hyperboloids were the kernel surfaces tested.

1. Determination of δ

Both hyperboloids and inverse hyperboloids require the parameter δ (Section II.F). Variation of δ makes considerable difference in the results. The effect of any value of δ on the shape of the quadric surfaces with respect to the entire model is related to the scale of the model. Hardy (1977) has indicated that the optimum value of δ in his investigations was also related to the distance between model points. The following expression

TABLE VI - Shepard's Formula with Inverse Distance Squared Weighting Function - Morro Bay

Number of model points	NPPR	RMS difference	Maximum positive difference	Maximum negative difference	Number of data points
37	4	2.83	9.51	-8.90	936
37	9	2.37	8.75	-9.09	936
37	25	2.36	8.38	-9.57	936
37	All*	5.00	14.62	-17.06	936
67	4	2.81	9.14	-8.87	936
67	9	2.31	6.01	-6.88	936
67	25	2.34	6.71	-9.00	936
67	All*	5.54	15.42	-19.90	936
98	4	2.58	9.33	-9.46	936
98	6	2.33	7.53	-7.84	936
98	9	2.18	7.75	-7.05	936
98	25	2.26	9.56	-8.40	936
98	56	2.72	10.57	-11.66	936
98	All*	6.58	15.50	-22.48	936

* Shepard's formula - All model points contributed to the weighted average.

was used to relate δ to the average density of the model points:

$$\delta = \frac{1}{2}\sqrt{\frac{D^2}{N}} \times 0.1 \times \text{NPPR} \qquad (17)$$

With this expression, the effect of δ on models of different scales will be similar as long as NPPR is the same. The tables in the following sections are expressed in terms of NPPR instead of the absolute value of δ.

A cone is a special case of hyperboloid where δ is zero. The tables for hyperboloid kernels include cones by listing NPPR as zero. A zero value of δ is not valid for inverse hyperboloids since the peak of an inverse hyperboloid increases to infinity as δ approaches zero.

2. Inverse Hyperboloid Kernels

For both data sets when δ was small (NPPR=5), the contours showed holes at the model points which were not indicated in the original data. The representation of the actual surface was very poor. Increasing NPPR to 10, 15 and 20 gave somewhat better results and the bottom trends were evident but the representation was still not good. With NPPR greater than 20, very steep slopes were created in large areas where no model points were chosen.

The statistical results using the Morro Bay data set are given in Table VII. The results became worse as more model points were added. The best results were considerably poorer than the best results from other methods, particularly the maximum differences.

TABLE VII - Multiquadric Analysis with Inverse Hyperboloid Kernels - Morro Bay

Number of model points	NPPR	RMS difference	Maximum positive difference	Maximum negative difference	Number of data points
37	5	4.99	4.71	-33.48	936
37	10	2.05	4.82	-21.09	936
37	15	1.59	4.56	-14.73	936
37	20	1.43	4.24	-10.90	936
67	5	6.11	5.50	-32.06	936
67	10	2.54	11.68	-21.15	936
67	15	2.69	17.74	-15.71	936
67	20	4.09	20.16	-15.60	936
98	5	23.85	2.35	-60.04	936
98	10	3.13	9.92	-23.96	936
98	15	3.98	21.97	-20.13	936
98	20	8.23	67.37	-33.72	936

3. Hyperboloid and Conic Kernels

Hyperbolic and conic kernels were evaluated on both data sets and NPPR was varied from zero to 25 for each set of model points. With 42 regularly spaced model points on the Monterey Bay data set, not much detail was evident but the general bottom trends were well represented for all values of NPPR. Increasing to 60 model points gave more variation with NPPR. For NPPR set to zero and one the results were very good. See Figure 14. The detail was improved and the bottom trends were still accurate. For NPPR set to 10 and 20, the results became progressively worse. Very steep slopes were generated which created invalid peaks and deeps in areas where no model points were chosen. The reason for these slopes is apparent when examining the magnitude of the coefficients. For NPPR=1, the mean coefficient magnitude was 0.33; for NPPR=20, the mean coefficient magnitude was 151.63. When NPPR was increased to 25, the system of equations became so ill-conditioned that it could not be solved. This is due to the increased flatness of the hyperboloids when NPPR becomes large. In areas where several model points are very close in order to represent sharp irregularities in the bottom, the flat hyperboloids centered at those points can't produce the detail required. Increasing to 90 model points produced similar results.

The statistical results from the Morro Bay data set are given in Table VIII. For small NPPR, the results became

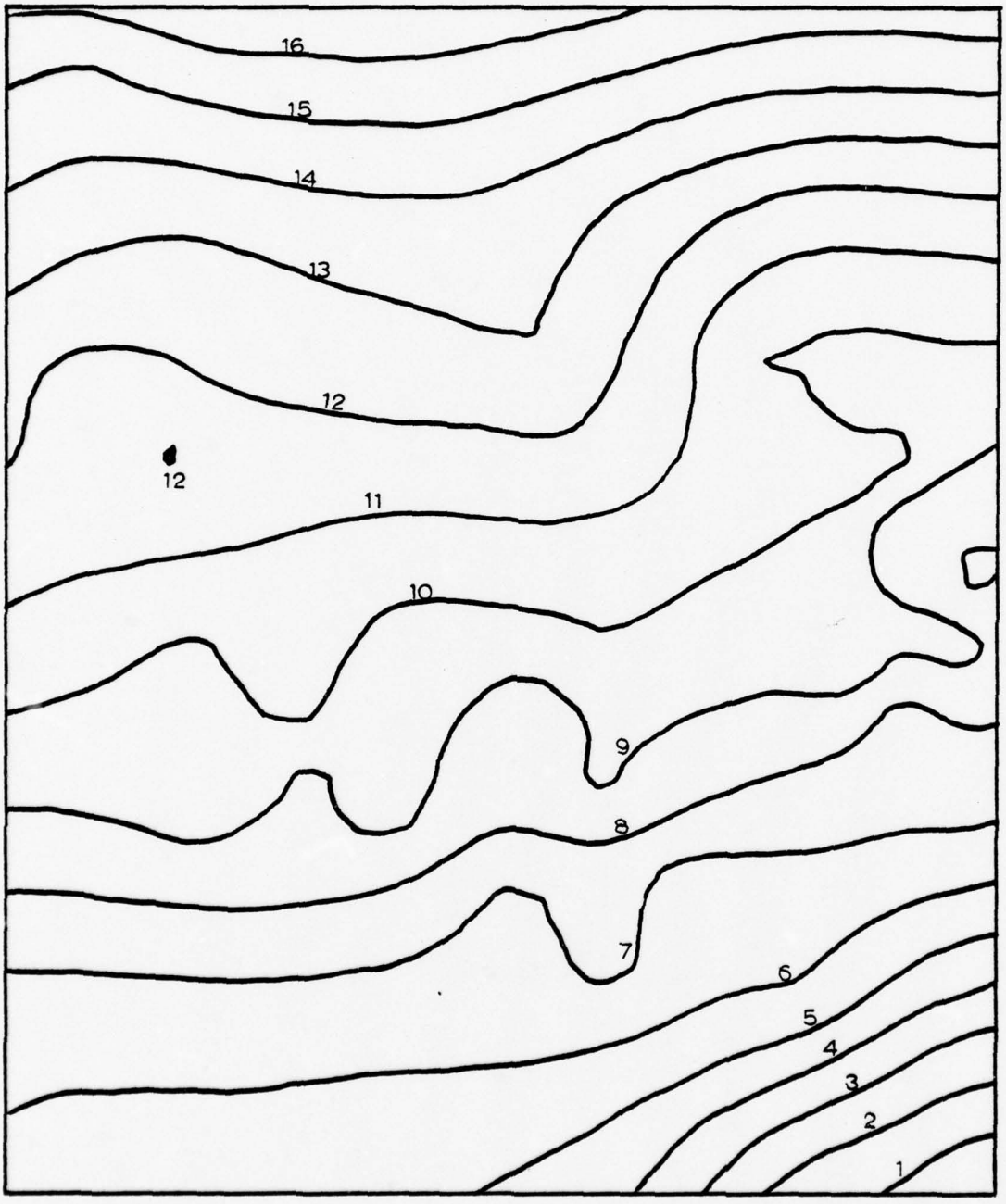

Figure 14 - 60 Point Multiquadric Model of Monterey Bay
(hyperboloid kernels)

TABLE VIII - Multiquadric Analysis with Hyperboloid and Conic Kernels - Morro Bay

Number of model points	NPPR	RMS difference	Maximum positive difference	Maximum negative difference	Number of data points
37	0	1.18	8.37	-6.59	936
37	1	1.14	6.00	-6.76	936
37	10	1.18	3.97	-6.92	936
37	25	1.24	3.90	-6.17	936
67	0	0.75	3.61	-3.09	936
67	1	0.78	3.59	-3.01	936
67	10	2.10	15.41	-6.79	936
67	25	12.04	62.50	-44.52	936
98	0	0.65	1.92	-2.14	936
98	1	0.68	2.06	-2.12	936
98	10	2.84	12.72	-14.11	936
98	20*	14.44	117.96	-43.61	936

* system couldn't be solved for NPPR=25

continually better as more points were added for greater detail. As the model points became more dense, the best results were acquired by using conic kernels (NPPR=0). For the original 37 regularly spaced model points, the best results were for small but non-zero NPPR. The contour comparisons reflected the model quality demonstrated by the statistics.

F. SUMMARY

A graphical comparison of the statistical results of the methods is given in Figure 15. Duchon's method with basis functions d^3 and $d^2 \log d$ gave only a fair representation of the bottom with regularly spaced model points. Additional model points did not improve the results so this technique was rejected. The basis function d logd, was introduced which gave good results (comparable to the multiquadric method) in one case and poor results in another. This was due to a dependence on the horizontal scale of the data. Independence of scaling for hydrographic survey modeling is very important since surveys are plotted at various scales. The method with basis function d logd is unacceptable for this reason.

Shepard's formula gave best results in modified form with about six model points in each radius of influence. The inverse distance weighting function was better than the square of the inverse distance. The results were

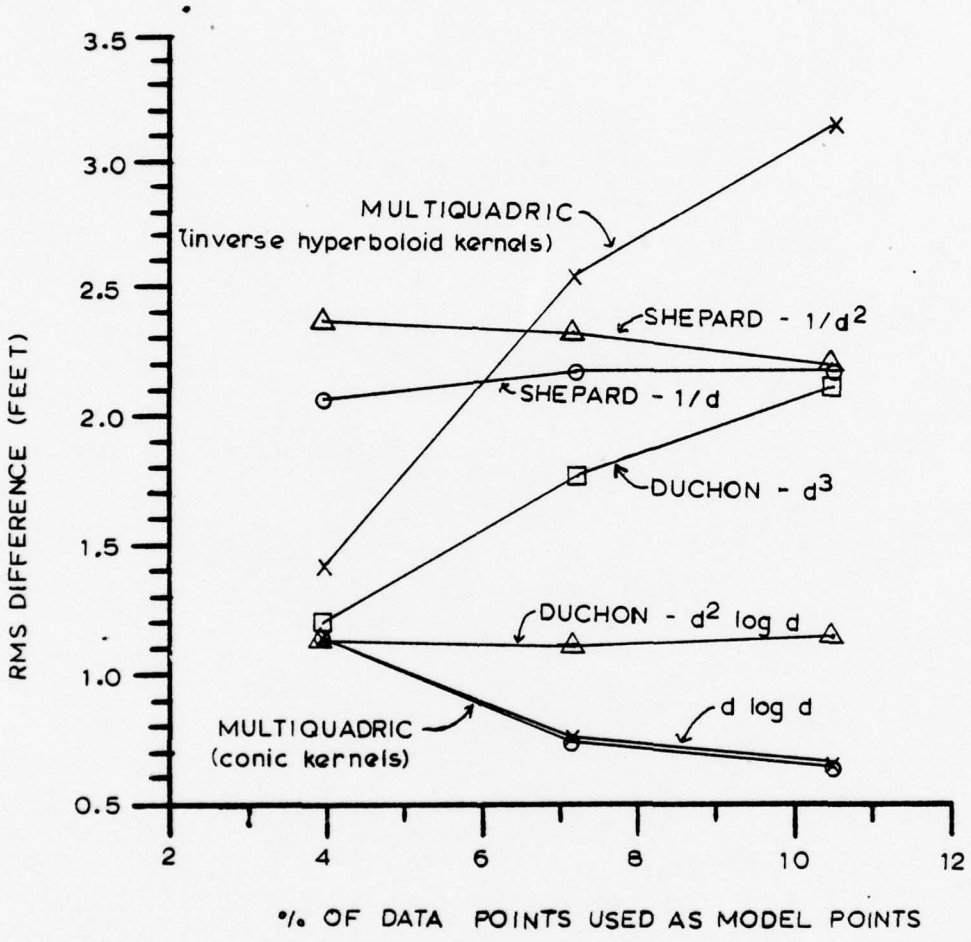

Figure 15 - Comparison of Modeling Methods

considerably worse than those of Duchon's or Hardy's methods. Improvement could not be gained by increasing the number of model points. For these reasons, Shepard's method was unacceptable.

Hardy's multiquadric analysis with inverse hyperboloids gave very poor results. For small δ holes were produced at the model points and the depths between model points were not accurate.

Of the methods tested, only multiquadric analysis with conic or sharply pointed hyperboloid kernels gave results which indicated that further tests were warranted. Depiction of detail is improved by adding more model points without adversely affecting the model in other areas and the method is independent of linear scaling.

VI. FURTHER TESTING OF MULTIQUADRIC ANALYSIS WITH CONIC AND HYPERBOLOID KERNELS

The results from the previous section showed that multiquadric analysis with conic or sharply pointed hyperboloid kernels was the only method tested that could meet the requirements of this application. Additional experimentation was done to determine the best procedures for selecting the model points and for joining models together at the boundaries. Tests were also run to determine how accurately the data sets could be represented with additional model points while still saving significant storage space.

A. SELECTION OF MODEL POINTS

The selection of the data points to be used for the modeling is a critical process in the development of the multiquadric model. Three models for selection of the points were tested using the Auke Bay, Alaska data set. All point selection was done manually but consideration was given to the difficulty in automating the process.

1. Regular Spacing Selection

In this method, data points from the survey were chosen at nearly even spacing without regard to depth,

bottom features, contour separation or any other factor. To avoid biasing, they were selected from a plot of record numbers rather than a plot of depths or depth contours. Additional points for more detail and accuracy were chosen for subsequent runs maintaining even spacing as much as possible without considering any factor except the horizontal distribution. The results of this procedure are presented in Table IX. The RMS differences were improved significantly when the number of model points was increased from 53 to 110 but the maximum positive differences were not improved. Additional densification of the model points produced little improvement in either the RMS differences or the maximum differences.

2. Iterative Selection

In the iterative selection process, the results of one model were used to eliminate some model points and select additional ones to produce a better model. After developing the model with the first set of points, the comparison of survey data points with the model was analyzed. Additional model points were selected wherever single point comparisons showed the largest differences or in areas where several points showed relatively large differences of the same sign. Model points which had very small associated coefficients were eliminated. A small coefficient indicates that the associated basis function has little effect on the model since it remains near zero within the modeled area. The model was then computed with the new set of points.

TABLE IX - Selection of Model Points with Even Spacing

Number of model points	NPPR	RMS difference	Maximum positive difference	Maximum negative difference	Number of data points
53	0	2.04	9.51	-5.64	1407
53	1	2.00	9.45	-5.78	1407
53	5	1.91	8.92	-6.39	1407
53	10	1.90	8.61	-7.03	1407
53	15	1.91	8.68	-7.66	1407
53	20	1.93	8.68	-8.10	1407
110	0	1.37	9.84	-4.25	1407
110	1	1.33	9.95	-4.71	1407
110	2	1.30	10.04	-5.02	1407
110	5	1.26	10.15	-5.46	1407
110	7	1.26	10.19	-5.60	1407
110	10	1.26	10.28	-5.76	1407
110	15	1.29	10.46	-5.97	1407
144	1	1.25	9.86	-4.26	1407
144	3	1.21	9.95	-4.66	1407
144	5	1.13	10.07	-5.41	1407
144	7	1.11	10.07	-5.58	1407
144	10	1.10	10.06	-5.76	1407
144	15	1.11	10.10	-6.01	1407

This procedure could be repeated until the desired accuracy was attained, the maximum number of model points to be used was reached, or the model accuracy no longer improved with further iterations. For this comparison of selection methods, the process was repeated until the number of model points was approximately the same as the maximum number used in the test of the regular spacing selection method.

Table X shows the results of these tests. In all tests, the best results were obtained when NPPR=0 (conic kernels). Both RMS and maximum differences improved significantly as the selection process was repeated. Two iterations yielded approximately the same number of model points as the maximum used in the regular spacing selection method.

Points related to features such as peaks, deeps or sharp changes in slope were chosen for the initial set of model points in these comparisons. Regular spaced points for the initial set were used in other tests with the iterative method. The results were good for both methods of initial selection. After a few iterations relatively few points from the initial set remained so the initial point selection method made little difference.

A comparison of model point selection by regular spacing and by iteration is shown in Figure 16.

TABLE X - Selection of Model Points by Iteration

Number of model points	NPPR	RMS difference	Maximum positive difference	Maximum negative difference	Number of data points
82	0	1.48	4.33	-5.52	1407
82	1	1.56	3.85	-5.50	1407
82	5	2.36	8.09	-9.43	1407
107	0	1.06	3.04	-3.29	1407
107	1	1.15	2.81	-3.32	1407
107	3	1.50	4.89	-4.82	1407
152	0	0.72	1.91	-2.58	1407
152	1	0.73	2.03	-2.72	1407

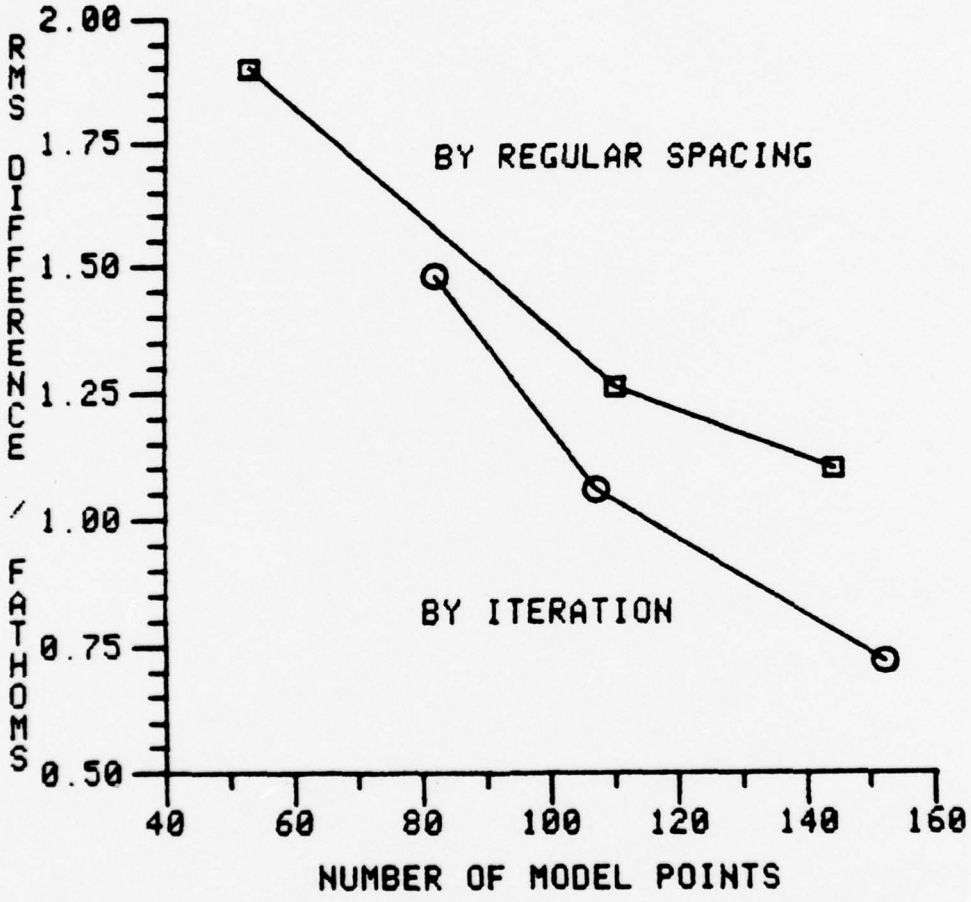

Figure 16 - Comparison of Model Point Selection Methods

3. Complete Selection by Topographic Feature

While using the iterative selection process, it was found that the additional points were selected where there were significant changes of slope or where there were large areas without any model points. This led to an attempt to select all the model points in one step based on the following criteria.

- Select points at peaks, deeps, ridges and where slopes change significantly.
- Select points to avoid leaving any large areas without model points as a result of the first criterion.

A test was done by choosing 145 points to model only half of the Auke Bay data set. The RMS difference was 0.88 and the maximum difference was -3.22. These results show that one-shot selection is not nearly as good as the iterative method and probably not much better than the regular spacing method.

4. Summary

The iterative selection method gave by far the best statistical results. It also required the most computer time. It would be adaptable to complete automation since the method for point selection has little subjectivity involved.

The regular spacing method would be easier to automate but it doesn't give good results when detail is required. The method of complete selection by feature doesn't give significantly better results than does regular spacing and the method would be difficult to automate.

B. MODEL JUNCTIONS

Agreement between two or more surveys which have a common boundary or cover a common area is a very important check on the quality of the surveys. Similarly, agreement between the models representing the surveys must be maintained to avoid ambiguity. The problem is even more acute when several models are joined together to represent a single survey. It would be desirable to represent an entire survey with a single model but in many cases this would be difficult due to the large systems of equations which would have to be solved to generate the model coefficients.

Hardy (1971) suggested a simple method of junctioning where common points on the boundary were used in adjacent models. This would assure that the models were in agreement at these points and if chosen at close intervals, the differences at intermediate points on the boundary would be relatively small. That method is not appropriate for this application since the data points are not along straight lines which could be used as boundaries. Common points on irregular boundaries could be used but this would complicate model boundary definition and storage.

Two other more appropriate methods were investigated for this application. Both use overlapping areas in the adjacent models rather than a common boundary.

The first method is analogous to the method of using common points on a boundary because the model points within the overlapping area are required to be the same for both models. A line in the middle of the overlapping area is chosen to delineate the areas of model usage. See Figure 17

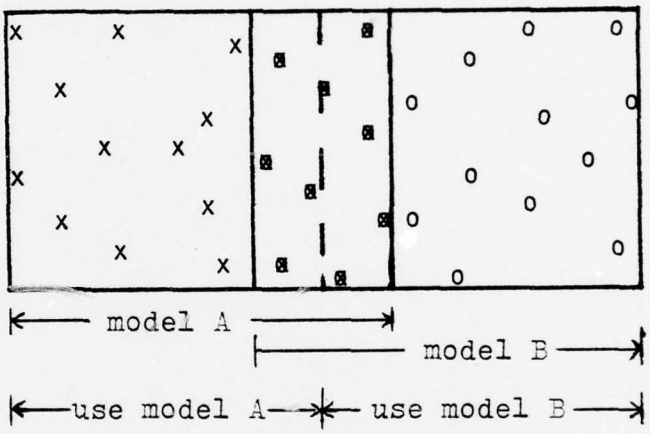

x - model points for model A
o - model points for model B
▪ - model points common to models A and B.

Figure 17 - Model Junctions by Overlap

This method could produce small discontinuities at the boundary.

The second method eliminates the discontinuity completel but requires more computation. The model points in the over lapping area are not required to be common in both models.

In this area, a weighted sum of the values obtained from each model is used. The weight, w, is determined by the Hermite Polynomial

$$w = 1 - 3s^2 + 2s^3$$

where s is the relative distance from the point of computation to the overlap area boundary. The value of s varies from one at the outer model boundary to zero at the inner boundary of the overlap area (see Figure 18).

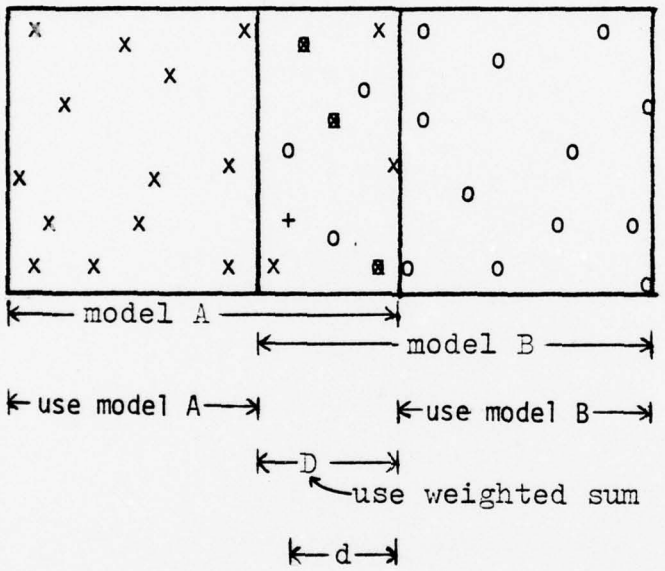

x - model points for model A
o - model points for model B
@ - model points common to models A and B
+ - point of computation

Figure 18 - Model Junction by Hermite Polynomial

The weight assigned to the model A value at the point of computation in Figure 18 is determined by using

$$s = \frac{D - d}{D} . \qquad (18)$$

The weight assigned to the model B value at the same point is determined by using

$$s = {}^{d}/_{D} \, . \qquad (19)$$

The sum of the resultant weights is always one. A plot of the Hermite polynomial is shown in Figure 19.

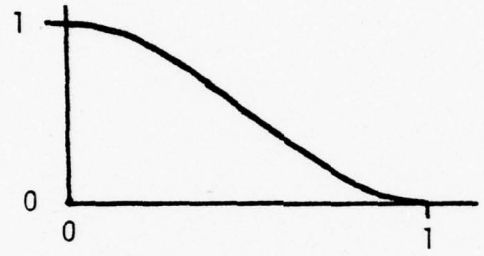

Figure 19 - Hermite Polynomial

Because the first derivative of this function is zero at s=0 and s=1, the transition from one model to an adjacent one will be smooth and continuous.

The Auke Bay survey was divided into two overlapping models as pictured in Figures 17 and 18. Each was modeled separately using the iterative method of model point selection. The two models were then joined by the two methods discussed above. The results are presented in Table XI.

Both junction methods showed improved results over the individual models since some of the largest errors were located near the outer boundaries of the models. The results with the polynomial method were only slightly better. Contour comparisons between the junction methods showed little difference. The possible discontinuity at the boundary when not using the Hermite polynomial was not apparent in the contours.

TABLE XI - Results of Model Junction

Model	Number of model points	RMS difference	Maximum positive difference	Maximum negative difference	Number of data points
West Side	175	0.321	1.397	-1.120	863
East Side	171	0.297	0.842	-0.854	825
Entire data set w/out Hermite Junction	290	0.306	0.842	-0.951	1407
Entire data set w/ Hermite junction	290	0.303	0.832	-0.951	1407

These results have shown that transition from one model to another can be done smoothly. The method using the Hermite polynomial is only slightly better than the method using common points in an overlapping area. When joining models without common points, e.g. two different surveys, the Hermite polynomial method will give a smooth non-ambiguous transition from one model to another.

C. MODEL REFINEMENT

Multiquadric analysis and the iterative method of model point selection were used to refine the models of all four data sets. Tables XII, XIII, XIV and XV give the statistical results of these tests. Figures 20, 21, 22 and 23 show the effect of each iteration on the RMS differences. The number of model points is expressed as a percentage of the number of data points represented. This is a direct indication of the storage savings attained by each model. All four figures show a similar trend. Initially, the results improve rapidly as the percentage of data points used in the model increases. The improvement then tends to level off and repeated iterations generate less improvement.

Contour plots of the final models for each data set are shown in Figures 24, 25, 26 and 27. Comparison of these with Figures 7, 8, 9 and 10 show the agreement with contours of the original data.

For the Monterey Bay model, an RMS difference of 0.2 fathoms and a maximum difference of -0.74 fathoms are good considering the irregularity of the bottom. These results were obtained using 17.2% of the data points as model points.

For the Morro Bay model, an RMS difference of 0.55 feet and a maximum difference of -1.58 feet are good considering that the depths range from 16 to 82 feet. This representation was made using only 15.7% of the data points. The allowable error specification (Section I.B) is one foot in the shallow end of this range and three feet in the deep end.

For the Auke Bay data set, an RMS difference of 0.30 fathoms and a maximum difference of -0.95 fathoms using 20.6% of the data points are good considering the steep slopes in the area. A horizontal positioning error of a few meters (within tolerance for the survey scale) could create several fathoms difference in many of the recorded depths.

Even though the range of depths in the Gulf Coast data set is small, and RMS difference of 0.30 feet and a maximum difference of -1.16 feet using 9.9% of the data points could be considered good. The allowable error (Section I.B) for these depths is one foot. There are places in the data set where crossline and adjacent soundings from multiple vessels disagree by as much as two feet. The model

representation tends to smooth out such discrepancies and this smoothing appears as relatively large differences in the statistics.

The Gulf Coast model gave the only case where a large δ (NPPR=50) gave much better results than smaller values. Only nine model points were used in that case. When more model points were added a small NPPR was required for good results.

TABLE XII - Monterey Bay Model Results

Number of model points	NPPR	RMS difference	Maximum positive difference	Maximum negative difference	Number of data points	Model point percentage
41	0	0.44556	1.87	-1.61	1315	3.1
69	0	0.42880	1.42	-1.37	1315	5.2
75	0	0.42228	1.42	-1.37	1315	5.7
102	0	0.32042	1.19	-1.02	1315	7.8
162	0	0.31449	0.98	-1.07	1315	12.3
185	0	0.25168	0.73	-0.91	1315	14.1
207	0	0.21952	0.77	-0.72	1315	15.7
226	0	0.20574	0.66	-0.74	1315	17.2

TABLE XIII - Morro Bay Model Results

Number of model points	NPPR	RMS difference	Maximum positive difference	Maximum negative difference	Number of data points	Model point percentage
37	0	1.18115	8.37	-6.59	936	4.0
67	0	0.75085	3.61	-3.09	936	7.2
98	0	0.64740	1.92	-2.15	936	10.5
106	0	0.67936	2.46	-1.87	936	11.3
135	0	0.57084	1.74	-1.66	936	14.4
147	0	0.55794	1.55	-1.58	936	15.7
144	0	0.55719	1.55	-1.58	936	15.4

TABLE XIV - Auke Bay Model Results

Number * of model points	NPPR	RMS difference	Maximum positive difference	Maximum negative difference	Number of data points	Model point percentage
82	0	1.47910	4.33	-5.52	1407	5.8
107	0	1.05619	3.04	-3.29	1407	7.6
152	0	0.71656	1.91	-2.58	1407	10.8
94W	0	0.79445	1.89	-3.13	863	10.9
144W	0	0.49843	2.36	-1.89	863	16.7
158W	0	0.39752	1.38	-1.88	863	18.3
175W	0	0.32183	1.40	-1.12	863	20.3
94E	0	0.75379	2.34	-2.59	825	11.4
141E	0	0.42834	1.74	-1.17	825	17.1
161E	0	0.34607	1.47	-1.26	825	19.5
171E	0	0.29729	0.84	-0.85	825	20.7
290H	0	0.30306	0.83	-0.95	1407	20.6

* W - West side of data set
E - East side of data set
H - East and west sides joined by Hermite Polynomial Method

TABLE XV - Gulf Coast Model Results

Number of model points	NPPR	RMS difference	Maximum positive difference	Maximum negative difference	Number of data points	Model Point percentage
9	0	3.18956	12.51	-2.68	1670	0.54
9	10	1.81510	7.93	-2.78	1670	0.54
9	20	1.03468	4.73	-2.40	1670	0.54
9	30	0.67701	2.81	-2.16	1670	0.54
9	40	0.55564	1.75	-2.05	1670	0.54
9	50	0.53023	1.73	-1.99	1670	0.54
9	75	0.55055	1.73	-2.42	1670	0.54
26	0	0.54879	2.04	-1.42	1670	1.56
26	1	0.55132	2.15	-1.40	1670	1.56
26	5	0.56410	2.30	-1.36	1670	1.56
26	10	0.58305	2.38	-1.39	1670	1.56
26	30	0.68191	2.50	-2.01	1670	1.56
47	0	0.48605	1.58	-2.28	1670	2.81

TABLE XV (cont)

Number of model points	NPPR	RMS difference	Maximum positive difference	Maximum negative difference	Number of data points	Model point percentage
47	1	0.51788	1.82	-2.37	1670	2.81
47	5	0.76205	3.44	-4.22	1670	2.81
47	10	1.23616	4.26	-7.04	1670	2.81
67	0	0.39612	1.58	-1.83	1670	4.01
86	0	0.38802	1.24	-1.16	1670	5.15
112	0	0.33139	1.24	-1.16	1670	6.71
125	0	0.32395	1.20	-1.04	1670	7.49
165	0	0.30310	1.12	-1.16	1670	9.88

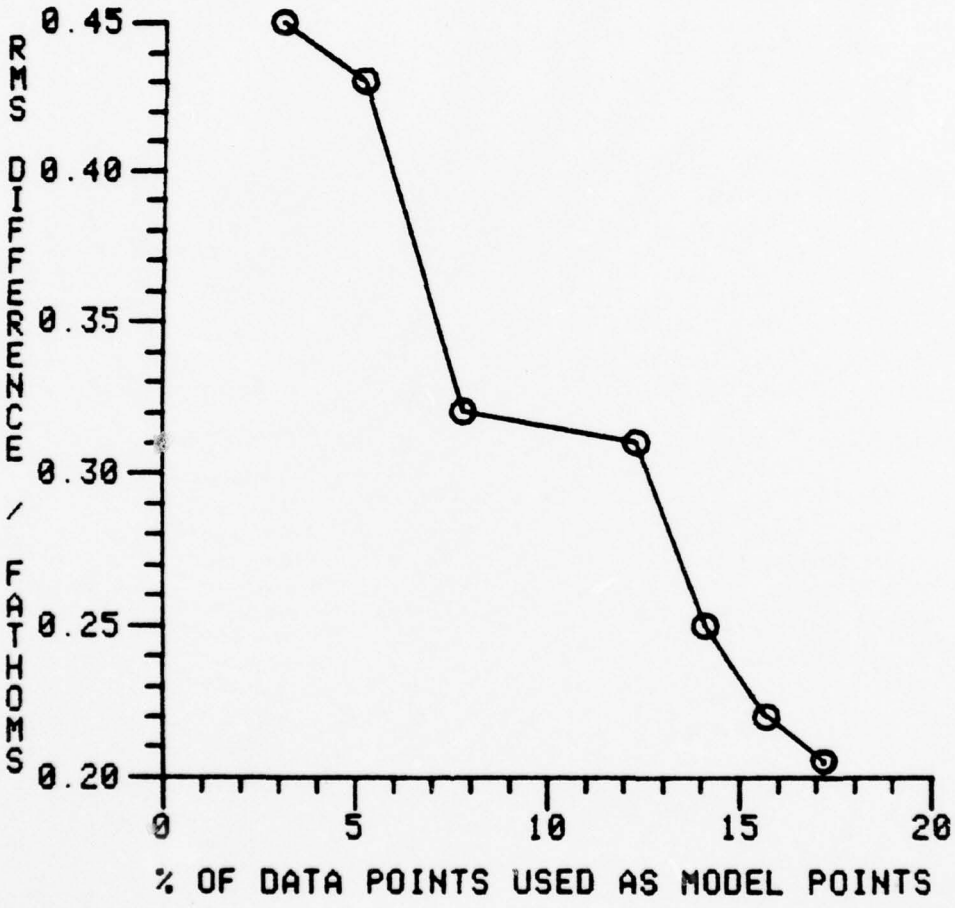

Figure 20 - Monterey Bay Model Results

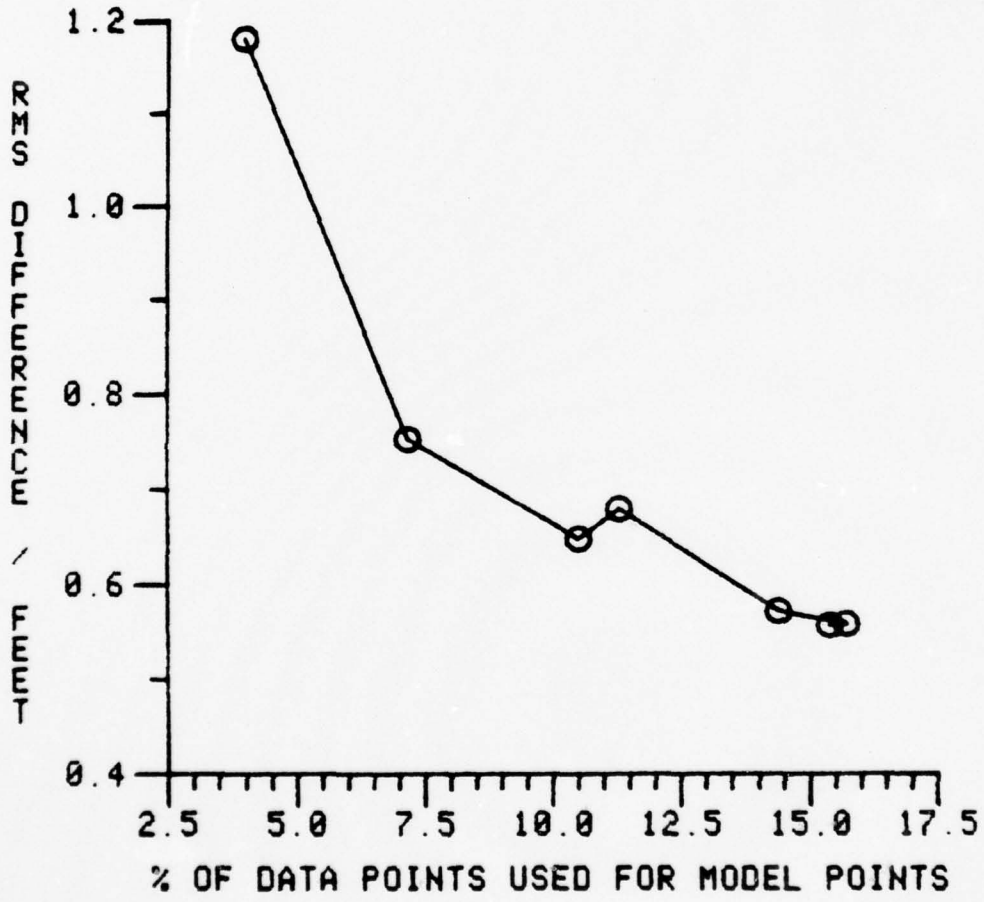

Figure 21 - Morro Bay Model Results

AD-A078 282 NAVAL POSTGRADUATE SCHOOL MONTEREY CA F/G 8/10
REPRESENTATION OF HYDROGRAPHIC SURVEYS AND OCEAN BOTTOM TOPOGRA--ETC(U)
SEP 79 A J PICKRELL

UNCLASSIFIED NL

2 OF 2
AD
A078282

END
DATE
FILMED
1-80
DDC

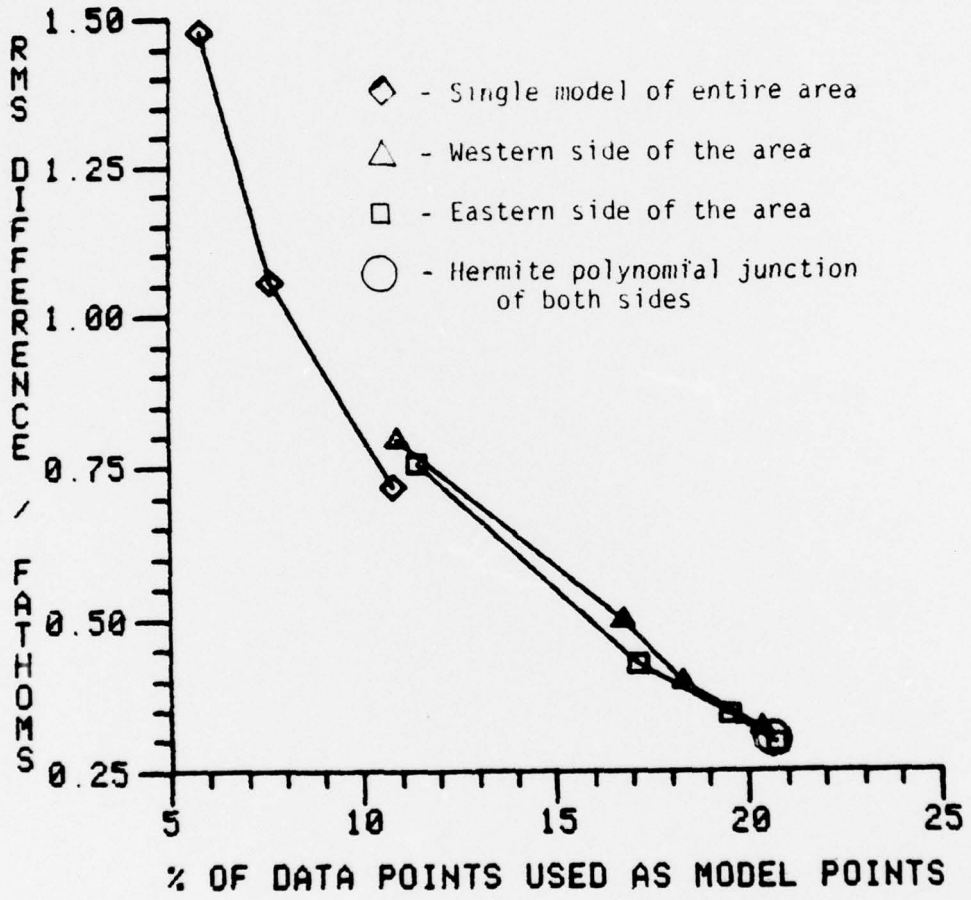

Figure 22 - Auke Bay Model Results

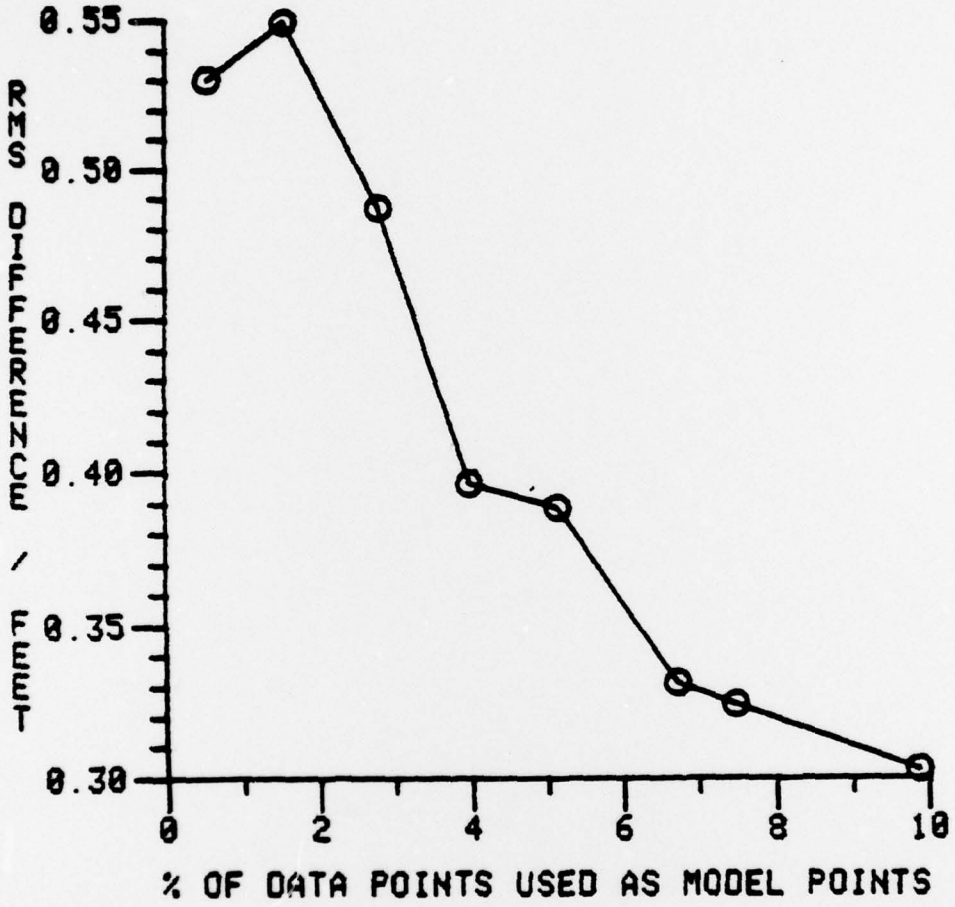

Figure 23 - Gulf Coast Model Results

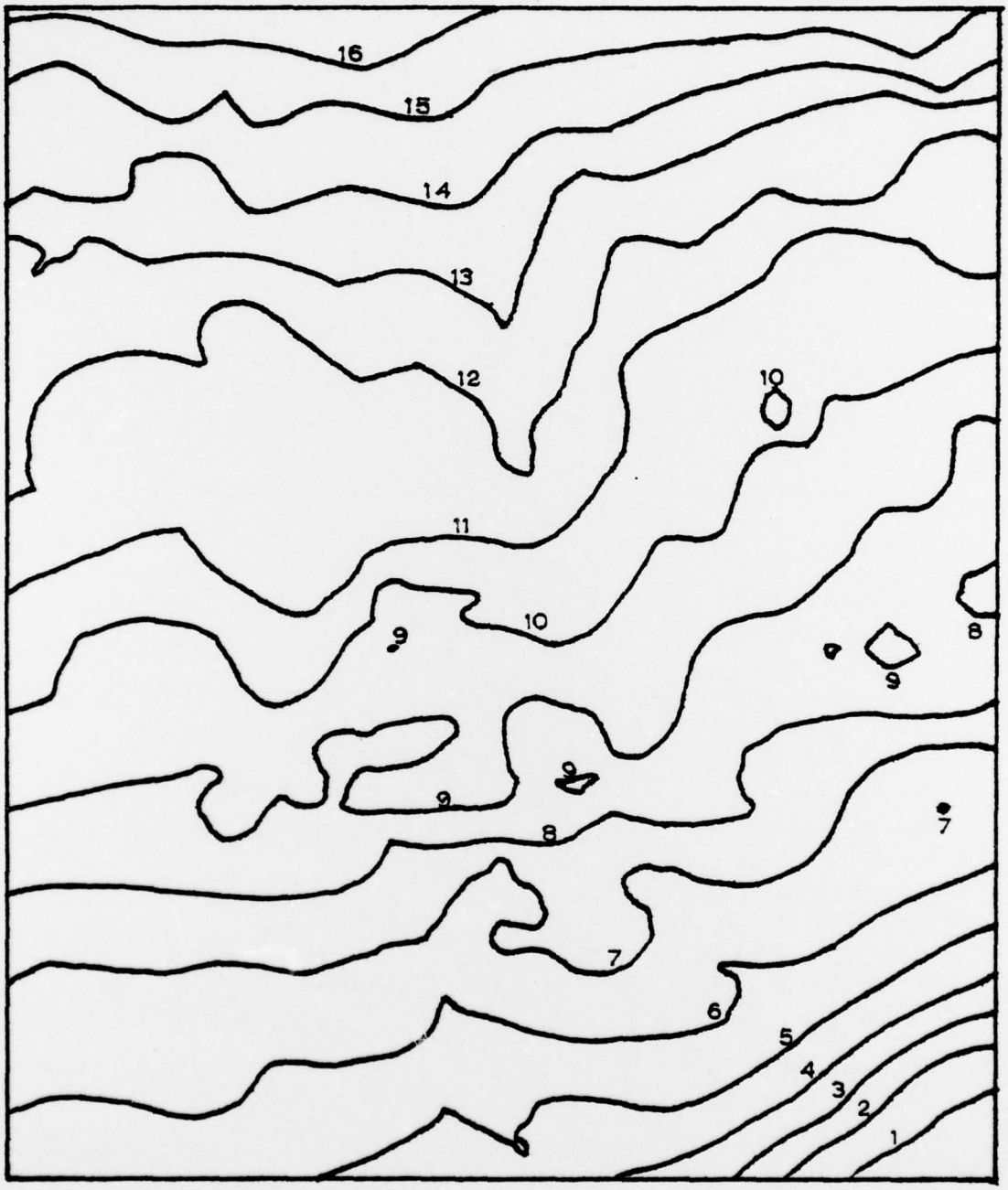

Figure 24 - 226 Point Monterey Bay Model Contours

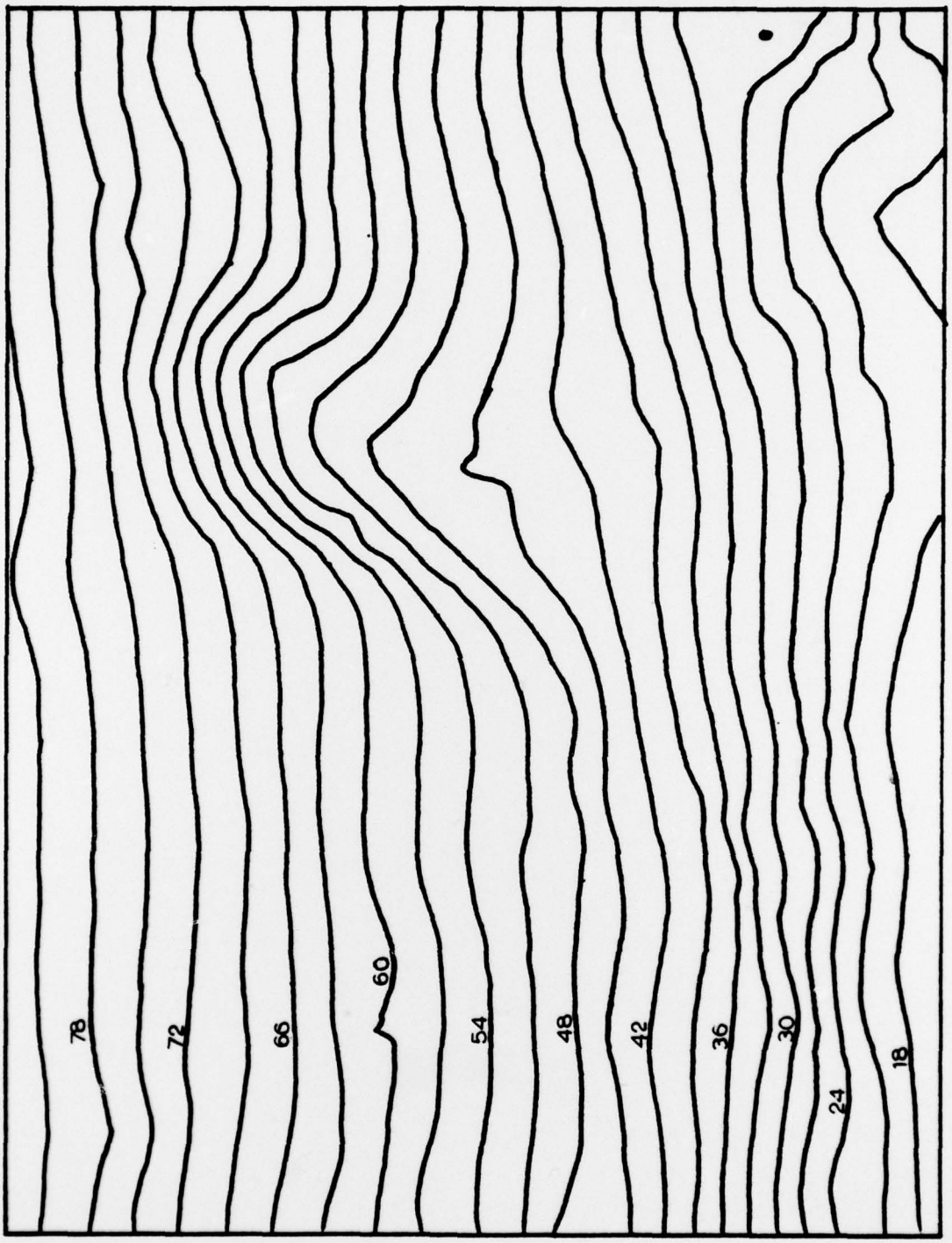

Figure 25 - 144 Point Morro Bay Model Contours

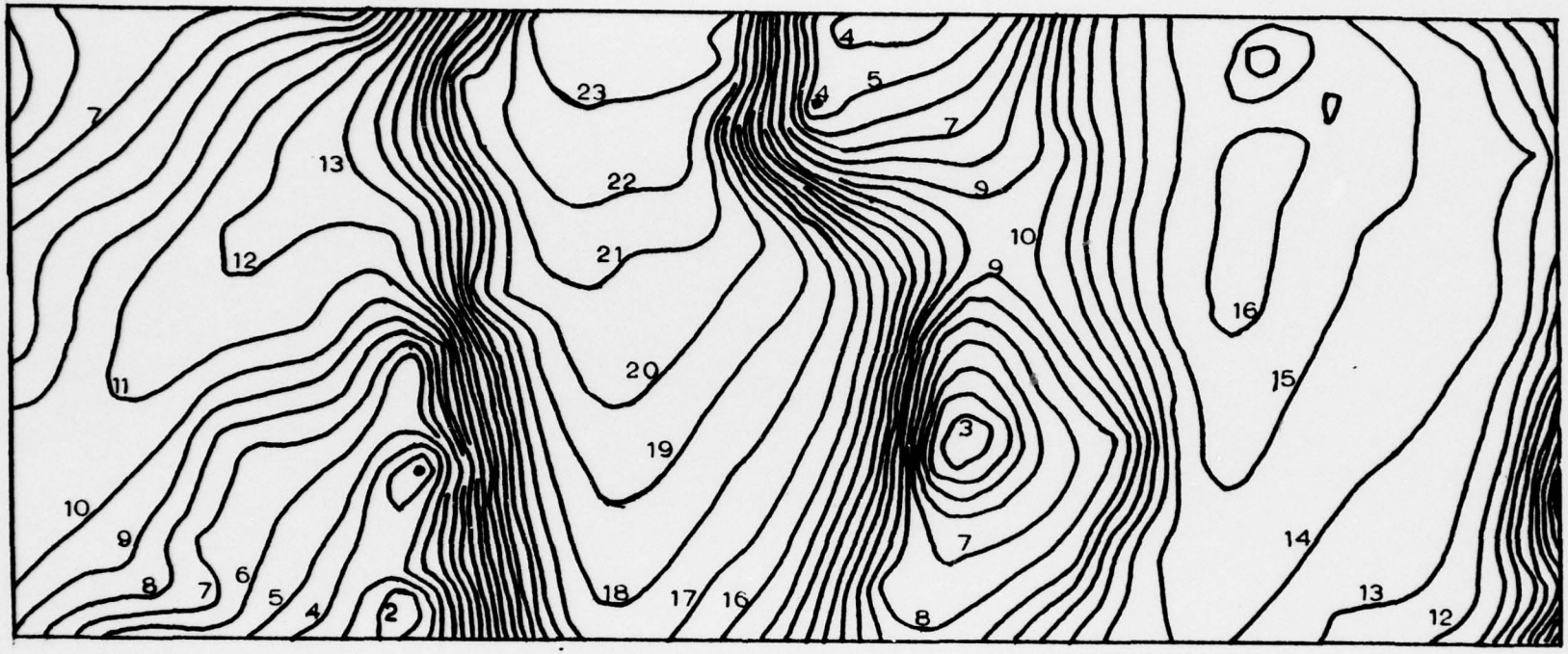

Figure 26 - 290 Point Auke Bay Model Contours

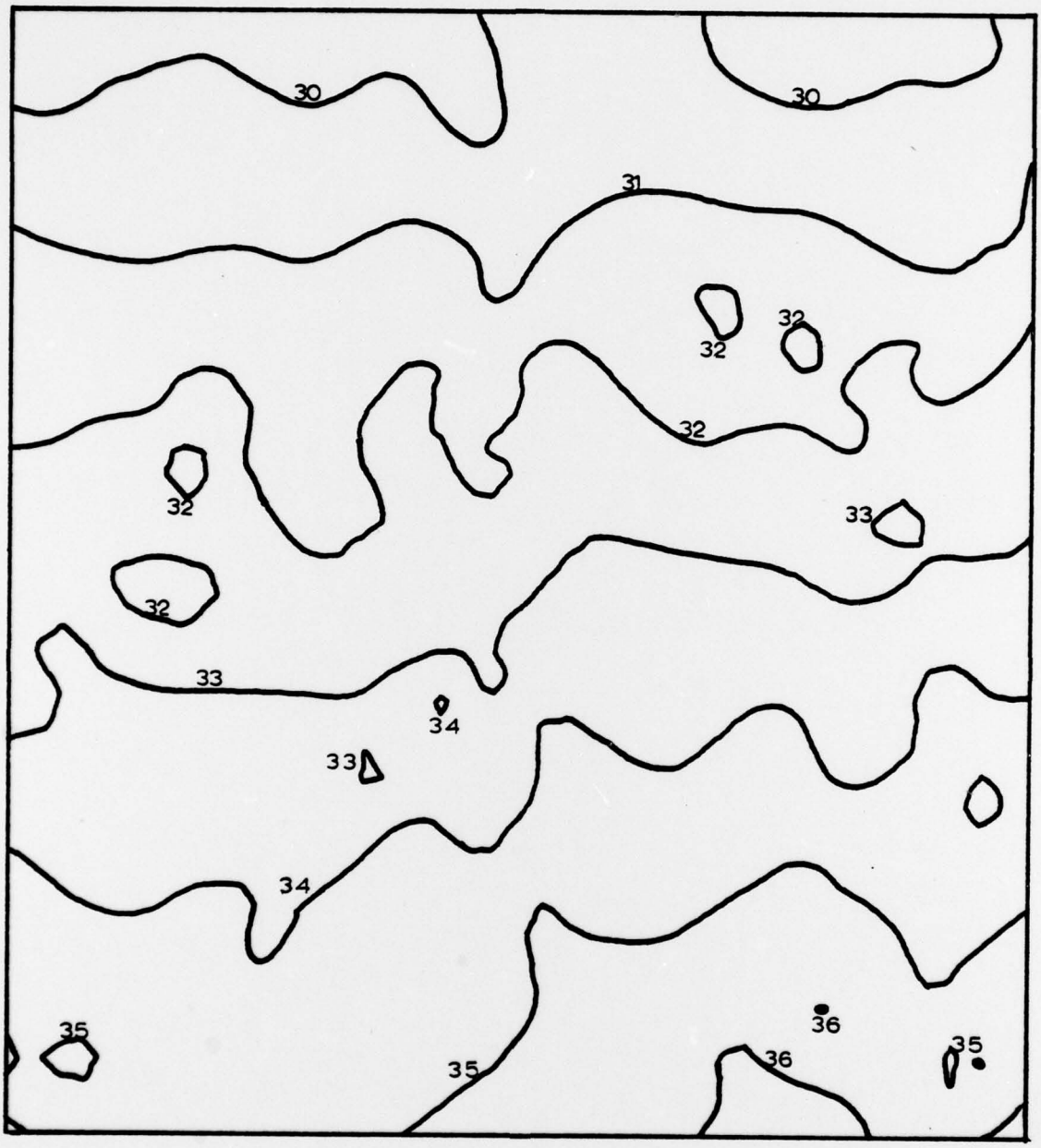

Figure 27 - 165 Point Gulf Coast Model Contours

VII. CONCLUSIONS

Of the methods examined, only Hardy's multiquadric modeling technique with conic kernels was found to be suitable for modeling hydrographic survey data. Polynomial, double Fourier series and finite element methods were rejected for reasons found in the literature. Duchon's method, Shepard's formula, and multiquadric analysis with inverse hyperboloid kernels were rejected as a result of tests presented herein.

Selection of model points for the multiquadric method is best performed by iteration. An initial set of model points may be chosen either by regular spacing or by bottom feature. Comparisons of the initial model with the survey data are used to select additional model points where there are large errors. Points with the smallest coefficients are eliminated from the set. A new model is computed and the process is repeated. This procedure can be repeated until the desired accuracy is reached or until additional iterations fail to produce increased accuracy. This method is considerably better than selecting regular spaced points and densifying them for more accuracy or selecting the maximum number of points at one time by examining the bottom features. The iterative method of model point selection is adaptable to automation since there is relatively little subjectivity involved.

Adjacent survey models or partial survey models can be joined to produce a continuous and unambiguous representation of the bottom in the junction area. The best method is to use a weighted sum of the model values in an overlapping area. The Hermite polynomial function should be used to produce the weights. If the two models contain common points in the overlapping area, a good junction can be made without computing a weighted sum. This method could produce a slight discontinuity along the boundary but it was not apparent in the test runs for this project.

The multiquadric technique with iterative selection of model points and Hermite polynomial junctions produced good models of four data sets. Approximately 20% of the survey data points were required for a model of Auke Bay, Alaska, where there is tremendous bottom irregularity. Only 10% of the data points were required for a model of the Gulf Coast where the bottom shows little variation. Approximately 15% and 17% were required for the Morro Bay and Monterey Bay models where there is more irregularity and moderately sloping bottoms.

LIST OF REFERENCES

1. AVCO Everett Research Laboratory, Inc., Airborne Hydrography System Limited Design Report, prepared for National Ocean Survey, contract no. 7-35373, January 1978.

2. Barnhill, R. E., "Representation and Approximation of Surfaces," Mathematical Software, vol. III, p. 69-120, Academic Press, 1977.

3. Czegledy, P. F., "Surface Fitting by Orthogonal Local Polynomials," Biometrical Journal, vol. 19, no. 4, p. 257-264, 1977.

4. Duchon, J., "Interpolation des Fonctions de Deux Variables Suivant le Principe de la Flexion des Plaques Minces," R. A. I. R. O. Analyse Numeriques, vol. 10, p. 5-12, 1976.

5. Duchon, J., "Fonctions-Spline à Énergie Invariante par Rotation," University of Grenoble, Research Report No. 27, 1976.

6. Franke, R., A Critical Comparison of Some Methods for Interpolation of Scattered Data, Naval Postgraduate School Technical Report NPS-53-79-003, 1979.

7. Gold, C. M., Charters, T. D., and Ramsden, J., "Automated Contour Mapping Using Triangular Element Data Structures and an Interpolant Over Each Irregular Triangular Domain," Computer Graphics, vol. 11, no. 2, p. 170-175, 1977.

8. Harder, R. L. and Dermarais, R. N., "Interpolation Using Surface Splines," Journal of Aircraft, vol. 9, p. 189-197, 1972.

9. Hardy, R. L., "Multiquadric Equations of Topography and Other Irregular Surfaces," Journal of Geophysical Research, vol. 76, no. 8, p. 1905-1915, 10 September 1971.

10. Hardy, R. L., "The Analytical Geometry of Topographic Surfaces," American Congress on Surveying and Mapping Proceedings, vol. 32, p. 163-181, 1972.

11. Hardy, R. L., "Analytical Topographic Surfaces by Spacial Intersection," Photogrametric Engineering, vol 38, p. 452-458, 1972.

12. Hardy, R. L., "Research Results in the Application of Multiquadric Equations to Surveying and Mapping Problems," Surveying and Mapping, vol. 35, p. 321-332, December 1975.

13. Hardy, R. L., "Least Squares Prediction," Photogrammetric Engineering and Remote Sensing, vol. 43, p. 475-492, April 1977.

14. Hopkins, R. and Mobley, W., "Recent Developments in Automated Hydrographic and Bathymetric Survey Systems in the National Ocean Survey," Offshore Technology Conference Proceedings, OTC3226, 1978.

15. International Hydrographic Bureau, Accuracy Standards Recommended for Hydrographic Surveys, Special Publication 44, Monaco, January 1968.

16. James, W. R., The Fourier Series Model in Map Analysis, Technical Report No. 1 of ONR Task No. 388-078, Contract Nonr-1228(36) for the Office of Naval Research, Northwestern University, April 1966.

17. Keller, M., A Study of Applied Photogrammetric Bathymetry the National Oceanic and Atmospheric Administration, in-house paper for the Coastal Mapping Division of the National Ocean Survey, 1976.

18. Krumbein, W. C., A Comparison of Polynomial and Fourier Models in Map Analysis, Technical Report No. 2 of ONR Task No. 388-078, Contract Nonr-1228(36) for the Office of Naval Research, Northwestern University, June 1966.

19. Meinguet, J., "Multivariate Interpolation at Arbitrary Points Made Simple," Zeitschrift für Angewandte Mathematik und Physik, vol. 30, no. 10, p. 292-304, 1979.

20. Moses, R. E. and Passauer, J. L., National Ocean Survey Automated Information System, paper presented at Auto-Carto IV sponsored by American Congress on Surveying and Mapping and the American Society of Photogrammetry in cooperation with the U. S. Public Health Service, 15 November 1979.

21. Peucker, T. K., Fowler, R. J., Little, J. J. and Mark, D. M., Digital Representation of Three-Dimensional Surfaces by Triangulated Irregular Networks, Technical Report No. 10, Office of Naval Research contract N00014-75-C-0886 (NR 389-171), 1976.

22. Poeppelmeier, C. C., A Boolean Sum Interpolation Scheme to Random Data for Computer Aided Geometric Design, Master of Science thesis, University of Utah, December 1975.

23. Umbach, M. J., Hydrographic Manual Fourth Edition, U. S. Department of Commerce National Oceanic and Atmospheric Administration, 4 July 1976.

24. Wallace, J. L., Hydroplot/Hydrolog Systems Manual, NOS Technical Manual No. 2, NOAA Handbook No. 24, U. S. Department of Commerce National Oceanic and Atmospheric Administration, September 1971.

25. Whitten, E. H. T., "Orthogonal Polynomial Trend Surfaces for Irregularly Spaced Data," Mathematical Geology, vol. 2, no. 2, p. 141-151, 1970.

DISTRIBUTION LIST

		No. Copies
1.	Chairman Code 68 Department of Oceanography Naval Postgraduate School Monterey, CA 93940	3
2.	Director Naval Oceanography Division (OP952) Navy Department Washington, D. C. 20350	1
3.	Office of Naval Research Code 480 Naval Ocean Research and Development Activity NSTL Station, MS 39529	1
4.	Dr. Robert E. Stevenson Scientific Liaison Office, ONR Scripps Institution of Oceanography La Jolla, CA 92037	1
5.	SIO Library University of California, San Diego P. O. Box 2367 La Jolla, CA 92037	1
6.	Department of Oceanography Library University of Washington Seattle, WA 98105	1
7.	Department of Oceanography Library Oregon State University Corvallis, OR 97331	1
8.	Commanding Officer Fleet Numerical Weather Control Monterey, CA 93940	1
9.	Commanding Officer Naval Environmental Prediction Research Facility Monterey, CA 93940	1
10.	Commander Oceanographic Systems Pacific Box 1390 Pearl Harbor, Hawaii 96860	1

11. Defense Documentation Center — 2
Cameron Station
Alexandria, VA 22314

12. Library Code 0142 — 2
Naval Postgraduate School
Monterey, CA 93940

13. Commanding Officer — 1
Naval Ocean Research and Development Activity
NSTL Station
Bay St. Louis, MS 39522

14. Commander — 1
Naval Oceanography Command
NSTL Station
Bay St. Louis, MS 39522

15. Commanding Officer — 1
Naval Oceanographic Office
NSTL Station
Bay St. Louis, MS 39522

16. National Oceanic and Atmospheric Administration — 1
Chief, Program Planning and Liaison, NC 2
Rockville, MD 20852

17. National Oceanic and Atmospheric Administration — 1
Chief, Marine Surveys and Maps, C3
Rockville, MD 20852

18. National Oceanic and Atmospheric Administration — 1
Director, National Ocean Survey, C
Rockville, MD 20852

19. LCDR David W. Yeager — 1
Field Procedures Officer
Atlantic Marine Center
439 W. York St.
Norfolk, VA 23510

20. National Oceanic and Atmospheric Administration — 1
Manager, Marine Data Systems Project, C31
Rockville, MD 20852

21. CDR Donald E. Nortrup — 1
Code 68Nr
Oceanography Department
Naval Postgraduate School
Monterey, CA 93940

22. Captain Wayne Mobley — 1
NOAA Ship RANIER
FPO
Seattle, WA 98799

23. Mr. Larry Mordock — 1
Pacific Marine Center, CPM3xl
1801 Fairview Ave., East
Seattle, WA 98102

24. LCDR Alan J. Pickrell — 5
3233 NE 105th Street
Seattle, WA 98125

25. Dr. Richard H. Franke — 2
Code 53 Fe
Department of Mathematics
Naval Postgraduate School
Monterey, CA 93940

26. Dr. R. W. Garwood — 2
Code 68Gd
Department of Oceanography
Naval Postgraduate School
Monterey, CA 93940

27. Dr. Dale F. Leipper — 1
Code 68Lr
Department of Oceanography
Naval Postgraduate School
Monterey, CA 93940

28. Dr. Rolland L. Hardy — 1
Professor in Charge, Geodesy & Photogrammetry
Department of Civil Engineering
Iowa State University
Ames, Iowa 50011

29. Professor Gregory M. Nielson — 1
Department of Mathematics
Arizona State University
Tempe, Arizona 85281

30. Professor R. E. Barnhill 1
Department of Mathematics
University of Utah
Salt Lake City, Utah 84112

31. Professor William J. Gordon 1
Department of Mathematics
Drexel University
Philadelphia, PA 19104

32. Steve Litts 1
Code HYAI
DMAHTC
6500 Brookes Lane
Washington, D. C. 20315

33. Maxim F. VanNorden 1
Code 8412
U. S. Naval Oceanographic Office
NSTL Station
Bay St. Louis, MS 39522